PB2000-106896

FINAL REPORT

PREDICTING THE ULTIMATE LOAD CARRYING CAPACITY OF LONG-SPAN PRECAST CONCRETE ARCH CULVERTS

by

M. Zoghi, Ph.D. and J. Hastings, P.E.
Department of Civil & Environmental Engineering

State Job No. 14595 (0)

A report of research studies conducted under the sponsorship of the Ohio Department of Transportation

June 2000

The University of Dayton

1. Report No.	2. Government Accession No.	3. Recipient's Catalog No.
OHIO/HWY-01/2000		

4. Title and Subtitle	5. Report Date
PREDICTING THE ULTIMATE LOAD CARRYING CAPACITY OF LONG-SPAN PRECAST CONCRETE ARCH CULVERTS	June, 2000
	6. Performing Organization Code
	8. Performing Organization Report No.
7. Author(s) Manoochehr Zoghi	10. Work Unit No. (TRAIS)
9. Performing Organization Name and Address The University of Dayton Department of Civil and Environmental Engineering & Engineering Mechanics 300 College Park Dayton, OH 45469-0243	11. Contract or Grant No. State Job No. 14595(0)
	13. Type of Report and Period Covered Final Report
12. Sponsoring Agency Name and Address Ohio Department of Transportation 1600 West Broad Street Columbus, OH 43223	14. Sponsoring Agency Code

15. Supplementary Notes

16. Abstract

In a previous full-scale live load test, partially sponsored by the Ohio Department of Transportation, conducted on a 36-ft precast reinforced concrete arch culvert the ultimate load carrying capacity could not be established due to the limited hydraulic jack's capacity. Furthermore, the earlier analysis was tailored to site-specific conditions. The objectives of this second phase of the research project were two fold. First, the failure mode of the test culvert was investigated utilizing a more rigorous analysis based on the modified CANDE finite-element computer program. Second, the soil-structure interaction characteristics of long-span precast concrete arch culverts were analyzed under a wide variety of site conditions using the previous full-scale load test results as a benchmark.

Accordingly, a finite-element model of the test bridge was developed using the modified CANDE computer program. Beam-column elements were utilized to model the actual structure, whereas quadrilateral (or triangular) elements were employed in modeling the surrounding soil including the backfill and fill cover, and foundation footings and bedding. The construction process was simulated by first analyzing the structure resting on its foundation with no backfill. Then, a series of soil lifts was added alongside the culvert until the process of backfilling around and over the structure was complete. The vehicular traffic load was replicated in the analysis by applying loads on the surface of the top layer of soil. The preceding analyses revealed that the ultimate load the arch culvert structure can withstand is approximately 340 kips. It was also determined that the high quality of soil compaction is paramount in the overall structural integrity and soil-structure interaction performance.

		No Restrictions. This document is available to the public through the National Technical Information Service, Springfield, Virginia 22161	
19. Security Classif. (of this report) Unclassified	20. Security Classif. (of this page) Unclassified	21. No. of Pages	22. Price

Form DOT F 1700.7 (8-72) Reproduction of completed page authorized

FINAL REPORT

Predicting the Ultimate Load Carrying Capacity of Long-Span Precast Concrete Arch Culverts

by

M. Zoghi, Ph.D. and J. Hastings, P.E.
Department of Civil and Environmental Engineering
The University of Dayton

June 2000

Prepared in cooperation with the Ohio Department of Transportation and the U.S. Department of Transportation, Federal Highway Administration.

TABLE OF CONTENTS

PAGE NO.

LIST OF FIGURES

LIST OF TABLES

EXECUTIVE SUMMARY

A full-scale live load test was conducted on a 36-ft span precast reinforced concrete arch culvert in October 1992. The soil-structure interaction analysis procedure of correlating the actual and predicted performance of this underground structure was the subject of study, partially sponsored by the Ohio Department of Transportation (ODOT), during the 1992-94 period.

Accordingly, an instrumented 36-ft span precast arch module was subjected to 10-kip load increments using a hydraulic jacking system on an actual job site. Structural performance was evaluated by means of continuously monitoring the vertical and horizontal deflections, along with crack widths, at various locations underside the unit, and surrounding earth pressures at the interface of structure and backfill soil. It was found that the structure performed satisfactorily and exceeded the design load and deflection requirements set forth by the AASHTO Specifications. The maximum deflection was less than one and one-half inches at 200-kip applied load increment. This 200-kip load was the limit of hydraulic jack's capacity and was seven and one-half times the design load. Furthermore, the unit rebounded to on-quarter inch deflection upon the load removal.

It was also verified that the finite-element analysis of the reference project using the modified CANDE computer program exhibited excellent correlation with the actual deflection readings as well as with soil pressure measurements. A complete compilation of data and an analysis based on actual measured conditions were published in the final

report entitled: "Predicting Performance of A Long-Span Precast Concrete Arch Culvert," submitted to the Ohio Department of Transportation in January 1994.

Although the structure greatly exceeded all performance requirements for highway loading, it could not be loaded to destruction due to the hydraulic jack's limited capacity. Thus, the failure mode of the test unit was not established. As part of the second phase of this research project, it was proposed to evaluate the soil-structure interaction behavior of the culvert under greater loads and verify the failure mechanism of the structure by using the modified CANDE finite-element computer program.

Furthermore, the analysis of the test unit was tailored to site-specific conditions. The arch-box shape units were installed on a continuous footing founded on rock. ODOT's 304 granular material was used for backfilling under controlled conditions. Since current ODOT and AASHTO requirements for culvert backfill are based on rules of thumb, the development of a design methodology for other site conditions was indispensable. Another objective of the present study was to investigate the soil-structure interaction characteristics of long-span precast concrete arch culverts under a wide variety of site conditions utilizing the previous full-scale load test results as a benchmark.

In light of above discussion, a finite-element model of the test unit was developed using the modified CANDE computer program. Beam-column elements were used to model the actual culvert structure, whereas quadrilateral (or triangular) elements were utilized in modeling the surrounding soil including the footings, foundation bedding, backfill, and fill cover. The soil-structure interaction analysis was accomplished in a step-by-step procedure, whereby the structure would initially be resting on its foundation with no backfill. Then, a series of soil lifts was added alongside the culvert representing the actual installation process. This incremental construction approach continued, adding one layer of elements at a time, until the process of backfilling around and over the structure was complete. The vehicular traffic loads was simulated in the analysis by applying loads on the surface of the top layer of soil. Evidently, as subsequent layers of soil are added to the assemblage of elements, simulating the actual construction process, they load the structure through their interaction. Thus, the behavior of the culvert is dependent on its interaction with the surrounding soil and can be simulated closely using a finite-element computer model, which provides a reliable and realistic basis for design.

The above finite-element computer model was utilized to investigate the two objectives of the present research project. First, a series of parametric studies was conducted to explore the effects of various soil properties on the structure. Numerous finite-element analyses were conducted based on the existing soil models within the CANDE software program including linear elastic, overburden dependent, Hardin, and Duncan, and another more recent Selig soil model. A comparison between the field data and the results obtained from the finite-element analyses revealed that the Selig's soil model with special soil characteristics was the most appropriate one for the test culvert project. Subsequently, parametric studies were conducted utilizing a matrix of soil types including SW95%, SW61%, ML95%, CL95%, and CL45% as backfill soil, at extreme ends beyond the backfill, below the foundation, and as cover soil above the structure in the many finite-element runs to investigate their interaction with the arch culvert bridge.

The preceding parametric studies of the soil-culvert entailed the evaluation of the mid-span displacement, earth pressure distribution, and settlements below the foundations. It was determined that by altering the soil properties below the foundation;

i.e., using less compacted soil, specifically ML49% soil type, causes very high displacements at the center of the structure. The earth pressure distribution was also influenced to some extent by varying the soil properties. In general, the well-compacted soils exhibited higher pressures at the haunches than the poorly-compacted soils (specially with respect to backfill soil and soil at the extreme ends).

The ML95% and CL95% soil types below the foundation supports exhibited the lowest net displacements. The SW95% soil had similar net displacement as the above two soil types, but its values increased more dramatically at the 350-kip load increment. Among the poorly-compacted soils, the SW61% fared surprisingly well. The CL45% performed poorly (with regard to net displacements) at the higher loads, while the ML49% performed poorly for the entire range of applied loads.

The ultimate load-carrying capacity of the culvert structure was also investigated based on the displacements at various locations, earth pressure distribution, bending moments, and thrusts, utilizing the modified CANDE finite-element computer program. First, the stresses at which yielding of reinforcing steel and crushing of concrete occurred were established in the laboratory. Then, a series of CANDE runs was conducted to determine the corresponding applied loads. It wad found that the steel yields at an applied load increment from 230 to 240 kips, while the concrete begins crushing at an applied load of approximately 250 kips.

Once the above loads are reached (i.e., the loads at which the yielding of steel and crushing of the concrete take place), the structure begins to form plastic hinges and behaves as a three-hinged arch. The hinges are located near the haunches and at mid-span. Evidently, the structure is still stable and capable of sustaining additional loads prior to ultimate failure. Consequently, the applied loads were incrementally increased to gauge the structural response with respect to displacements, moments, and soil pressures. It was observed that as the applied load increased beyond the 250-kip increment, the values of displacements, moments, and earth pressures increased rapidly to a maximum level and then abruptly tapered off. The point, at which sudden change of structural response took place, was considered to be the ultimate failure. Based on this methodology and the concept of soil-structure interaction, the ultimate load that arch culvert structure can withstand is approximately 340 kips. This is an impressive 13 times greater than the design load of 26 kips.

I. INTRODUCTION

The soil-structure interaction analysis procedure of correlating the actual and predicted performance of a long-span precast reinforced concrete arch culvert was the subject of study under project number 93438 (ODOT's agreement number 7113) during the 1992-94 period (1). An instrumented 36-ft span arch-box precast bridge unit was subjected to increments of loads using a jacking system on an actual job site. Structural response via vertical and horizontal deflections, surrounding soil pressures, and crack widths were continuously monitored while load was being applied in 10-kip increments. The structure performed satisfactorily and exceeded the design load and deflection requirements set forth by the AASHTO Specifications. Maximum deflection was less than one and one-half inches at 200-kips of applied load. This 200 kip load was the limit of the hydraulic jack's capacity and was seven and one-half times the design load. The structure rebounded to one-quarter inch deflection when the load was removed.

The finite element analysis of the reference project using the modified CANDE program exhibited excellent correlation with actual deflection readings as well as with soil pressure measurements. A complete compilation of data and an analysis based on actual measured conditions were published in the final report entitled "Predicting Performance of A Long-Span Precast Concrete Arch Culvert," submitted to the Ohio Department of Transportation (ODOT) in January 1994 (1).

Although the structure greatly exceeded all performance requirements for highway loading, it could not be loaded to destruction because of the hydraulic jack's limited capacity. Thus the failure mode of the test unit had yet to be determined. As part of the second phase of this research project, it was proposed to evaluate the soil-structure interaction behavior of the culvert under greater loads and verify the failure mechanism of the structure by using the modified CANDE finite element computer program (2).

Furthermore, the analysis of the reference project was tailored to site-specific conditions. The arch-box shape units were installed on a continuous footing founded on rock. ODOT's 304 granular material was used for backfilling under controlled conditions (3). It is well known that current ODOT and AASHTO requirements for culvert backfill are based on rules of thumb (4). It is therefore necessary to develop design methodology for a wide variety of site conditions using the reference full-scale load-test program as a benchmark. In general, the behavior of a buried structure, to some extent, depends on its interaction with the soil surrounding the structure as backfill; fill cover, and foundation bed (5). The results of the second phase of investigation are summarized in this report.

II. OBJECTIVES OF STUDY

The objectives of this second phase of the research project were two-fold. First, the soil-structure interaction characteristics of long-span precast concrete arch culverts were investigated under a wide variety of site conditions using the previous full-scale load test results as a benchmark. Second, the failure mode of the test culvert was investigated utilizing a more rigorous analysis based on the modified CANDE finite element computer program.

III. COMPUTER ANALYSIS

The computer model of the reference full-scale load-test, generated by the modified CANDE program proved to be a reliable method to study the performance of buried structures. The CANDE program is a versatile code, which permits the analysis of culverts beyond the conventional elastic range into the plastic state. The analysis is accomplished in a step-by-step procedure, whereby the structure initially rests on its foundation with no backfill. Then, a series of soil lifts is added alongside the culvert representing the actual installation process. This incremental construction approach is continued, adding one layer of elements at a time, until the process of backfilling around and over the structure is completed. The vehicular traffic loads are simulated in the analysis by applying loads on the surface of the top layer of soil. As subsequent layers of soil are added to the assemblage of elements, simulating the actual construction process, they load the structure through their interaction (6). Incidentally, the behavior of the culvert is dependent on its interaction with the surrounding soil and can be simulated closely using a finite element computer model, which provides a reliable and realistic basis for design.

The above procedure was adopted to investigate the structural response to soils possessing different material and engineering properties. Several soil models were employed in the computer analysis to verify their effects on the reference arch culvert structure. The results of this study are described herein.

1. Soil Models Used in the Computer Analyses and Parametric Studies

Traditional methods of load distribution on a culvert were ordinarily based on empirical relations, limited to the database upon which they were built. Thanks to the advent of computer technology, the more sophisticated finite element solutions can be used as a rigorous analytical tool for evaluating the soil and culvert together into the boundary value problem. CANDE has been recognized as the most advanced soil-structure interaction finite element code to date, which encompasses all the structural features as well as state-of-the-art geotechnical engineering data. There are a host of soil models in the CANDE program, which can be called upon for various soil-structure interaction analyses. A listing of the soil models follows, along with a brief description of their relevance to the current study. Further more, the engineering properties of the soil models are tabulated in Appendix A.

Soil models used in the computer analyses:

a) Linear elastic

b) Overburden dependent

c) Hardin

d) Duncan

e) Selig

Specifically, Selig's parameters for in-situ soil and special materials turned out to be the most appropriate ones for the test culvert project (7). A series of parametric studies was conducted by varying the soil properties in the following locations:

a) The in-situ foundation soil below the structure (soil below foundation);

b) The soil, which is placed and compacted adjacent to the legs of the structure (backfill soil);

c) The in-situ soil at the sides of the structure beyond the backfill soil described above (soil at extreme ends);

d) The soil placed and compacted over the top of the structure (cover soil).

The parametric studies utilized the six different types of soils listed above along with their associated engineering properties (see Table 1).

Table 1. Soil Types and Their Associated Engineering Properties.

1	SW95%	Coarse-grained gravelly sand soil at 95% of maximum dry density (95% compaction)
2	SW61%	Coarse-grained gravelly sand soil simply dumped in place (61% compaction)
3	ML95%	Silty soil at 95% compaction
4	ML49%	Silty soil dumped in place (49% compaction)
5	CL95%	Clayey soil at 95% compaction
6	CL45%	Clayey soil dumped in place (45% compaction)

The effects of the six different soil types were investigated with respect to four different locations listed above to explore the structural response concerning the displacement at mid-span, earth pressure distribution at the haunches, and net settlement below the foundation. The parametric studies also utilized two other soil types: the site soil from the previous research project and the CANDE representation of this soil (CANDE B.M.). The engineering soil properties of this CANDE benchmark soil (CANDE B.M.) are listed in Appendix B.

2. Structural Details

A schematic diagram of the test precast concrete arch culvert unit is shown in Figure 1. Figure 2 shows the shop drawing for this structure (8). The crown is laid out with a radius of 40ft, the haunches possess a radius of 4 ft each, the thickness of the top segment is 12 inches, the sidewalls are 14 inches thick, and the transitional curves at the haunches vary in thickness as depicted in Figure 1 (Appendix C). The unit is reinforced using two mats of reinforcing steel on the inside and outside faces as illustrated in Figure 2 (Appendix C).

3. <u>Finite Element Model</u>

The finite element computer program used for the soil-structure analysis of the current project is based on plane-strain methodology, i.e., the culvert and surrounding soil are considered as a long; prismatic configuration with no variation in the loading along the longitudinal axis. In addition, deformation in the longitudinal direction is prohibited, maintaining similar transverse deformation for every cross section under consideration. Consequently, the three dimensional system is reduced into a single plane representative cross-section encompassing: culvert size and shape, wall section properties and material properties per unit length, soil geometric and material properties for various zones, and different loading configurations including the self-weight of the soil as well as live load pressures due to construction equipment and vehicular traffic (9).

The types of basic elements in a finite element code are central, making up the building blocks of the soil-structure system (10). These basic elements in the CANDE program are:

a) Beam-column elements, used for modeling the culvert structure. A typical assemblage of beam-column elements for the reference culvert unit is represented in Figure 3 (Appendix D). It is noted herein that each beam-column element is a straight, line-shaped element, possessing a node at each end. Total of 32 elements and 33 nodes make up this particular structure. Three degrees of freedom: i.e., two translational and one rotational, are associated with each node.

b) Quadrilateral (or triangular) elements are utilized in modeling the surrounding soil including the footings, foundation bedding, backfill, and fill cover. An assemblage of soil elements, representing the in-situ characteristics of reference project, is depicted in Figure 4. A quadrilateral element contains four external nodes at the element vertices, possessing two translational degrees of freedom per node. Also shown in Figure 5 is the nodal numbers associated with the above elemental assemblage. It is worth noting that the nonlinear soil characteristics are portrayed in these elements owing to availability of several options of stress-strain models as well as internal degrees of freedom.

c) Interface elements, to be adopted for special interface problems. This will be the subject of future research.

4. The Ultimate Load-Carrying Capacity of the Arch Structure

The CANDE program was utilized to determine the maximum load carrying capacity of the arch culvert structure. Using the CANDE Benchmark (CANDE B.M.) soil data, several different test values were computed as the applied load was incrementally increased. The test values included: 1) displacements at various locations, 2) normal soil pressure, 3) moment, and 4) thrust.

It was assumed that the arch culvert structure would behave elastically up to a certain point and then go into the plastic state with values increasing more rapidly. The values in the plastic state would increase up to a maximum point and then taper off quickly; failure of the structure would occur at this maximum point. The upper limit of the elastic range was established by running the CANDE program at 200 kips of applied load and computing the steel tensile stress at which yielding occurs and the concrete compressive stress at which crushing of the concrete begins to occur (See Figure 6, Appendix E). These values were 8370 psi and 7175 psi, respectively. Using these two values as a maximum stress, the applied loads could be gradually increased until the stress reaches the maximum. The test values could then be recorded and plotted.

With the structure behaving in the plastic state, loads were gradually increased and then the test values (from the CANDE program) were recorded. The applied load was increased up to the maximum and beyond to establish a good pattern of the increase and then sudden decrease in the test values. These test values were plotted for a wide range of applied loads. Many of these plots are also included in this report (Appendix G) to illustrate the behavior of the arch culvert structure under various construction and vehicular loading.

IV. PARAMETRIC STUDIES

A series of parametric studies was conducted by varying the soil properties in four different locations (see Figure 7). The four locations were 1) soil below foundation, 2) soil at backfill, 3) soil at extreme ends, and 4) soil at the top of culvert. Six different types of soils were considered in the analyses: SW 95%, SW 61%, ML95%, ML49%, CL95%, and CL49%. These are referred to as the test soils. The site soil and its CANDE representation were also included. The effects of different soil types were analyzed to determine the structural response with respect to mid-span displacement, earth pressure at the haunches, settlement below the foundation, and the net displacement of the structure. The results of the parametric studies are described in this section.

1. Displacement at Center

A. <u>Backfill Soil</u>

The effect of site soil on the mid-span displacement was somewhat different than the test soils (i.e., the site soil caused about 1/3 to 1/2 less displacement than the test soils) as shown in Figure 8. The CANDE approximation of the mid-span displacement averaged 30% to 50% higher than the site displacement. At 200 kips of load, the site displacement was 1.50" and the CANDE displacement was 1.75". The displacement obtained from based on the CANDE test soils were clustered fairly close together at 1.5 to 3 times greater than the site values. The poorly-compacted soils exhibited the highest displacements, but they were only slightly larger than the well-compacted soils. Of the well-compacted soils, the CL95% had the highest displacements, the ML 95% had 2nd highest, SW 95% 3rd highest. The site soil must have had excellent compaction and/or the CANDE program overestimates these deflections. The displacement curves representing the site soil did not correlate closely with the other curves exhibiting the results from the designated test soils.

B. Soil above the culvert

There was a similar trend regarding the cover soil, as depicted in Figure 9. The mid-span displacement associated with the site soil was 1/2 to 3/4 of the test soils. The CANDE approximation of the site displacement (CANDE B.M.) averaged 30% to 50% higher than the actual site displacements. At 200 kips of load, the site displacement was 1.40" and CANDE was 1.70". The CANDE test soils were clustered very close together at 1.25 to 2.5 times greater than the site. There was not much distinction here between the well-compacted and poorly-compacted soils. The worst performing test soil was the SW 61%. The best performing of these test soils were the SW95% and the ML95%. Test soils were very close to CANDE (B.M.).

The soil type and compaction rate for soil above of the culvert seem to have the least effect on the displacement when compared to soils at other locations near the culvert. It is standard practice to utilize sand and gravel as backfill and on top of the culvert. There should be more emphasis placed on achieving high quality compaction, which would reduce displacements. The minimal effect of different soil types above the culvert on the center displacement seems to indicate that silts and clays could be used as fill on top of the culvert (in isolated cases) if they are compacted well. One must be careful not to use highly expansive clays here, especially under roadway pavement. This is typically applicable beyond the roadway pavement, since most public agencies require granular backfill around and above a roadway culvert.

C. Soil at Extreme Ends

The mid-span displacement of the structure, in conjunction with the site soil, was much lower than those associated with the test soils (about 1/4 to 1/2 of the test displacements). The CANDE approximation of the site displacement averaged 30% to 50% higher than actual site displacement (see Figure 10). At 200 kips of load, the structure's center displacement, associated with the site soil, was 1.50" whereas the CANDE calculated it at 1.75". The displacement results obtained from CANDE based on the test soils were clustered fairly close together, again at 2 to 4 times greater than the site soil. The poorly-compacted soils showed the largest displacements with the following three soil types: CL45%, ML49% and SW61%, having very similar characteristics. The structure with well-compacted soils had slightly smaller displacements with the SW95% having the lowest one, the ML49% the second lowest, and the CL95% the highest displacement of the well-compacted soils.

D. Soil Below Foundation

The structure experienced the lowest center displacement with the site soil as shown in Figure 11. The CANDE (B.M.) closely approximates this site soil. The CANDE computer program calculated a wide range of displacements for the structure with the test soils, varying between 2 to 30 times greater than the site soil displacements. The structure experienced the largest displacements with ML49% soil type, which ranged from 4" to 7" at the center. These displacements are considered totally unacceptable for a typical arch culvert installation. The structure exhibited the second highest displacements with SW61%, which ranged from 2" to 4" (still considered too high). The structure with CL45% soil had the third highest displacements, which ranged from 1" to 3". The well-compacted soils had displacements fairly close to each other. The SW95% had the lowest displacements with ML95% at a very close second and CL95% at a close third. The CANDE (B.M.) and the three well-compacted soils closely approximated the site soil.

Compaction of the foundation soil needs to be emphasized very strongly. The compaction rate for the soil below the foundation has a very profound effect on the displacements at the center of the structure. The poorly-compacted foundation soils (ML49%, SW61% and CL45%) caused very high displacements. The ML49% in particular performed very poorly with displacements ranging from 4" to 7". It is important to realize that the foundation soil should be properly compacted, in accordance with the specifications, in order to prevent any future settlement.

2. Earth Pressure Distribution at the Haunches

A. <u>Soil at backfill</u>

The site soil and the CANDE (B.M.) soil exert the highest earth pressures on the haunches when compared to the other soils as depicted in Figure 12. Pressures range from 5 to 55 psi. Of the 3 poorly-compacted test soils, none of them show any significant earth pressure at the haunches. This would seem to indicate that no (or very little) soil-structure interaction has been achieved. Of the 3 well-compacted test soils, the SW95% has the highest earth pressure at the haunches, which is roughly 2/3 to 3/4 of the site and CANDE B.M. values. Pressures range from 3 to 32 psi. Site soil must have had excellent compaction in order to achieve such high earth pressure distribution.

B. Cover Soil

Figure 13 shows a trend similar to the mid-span displacement for the soil above the culvert. The type of soil and compaction rate for soil at the top did not seem to have significant influence on the earth pressure distribution at the haunches (the different soil types all follow essentially similar trend). The site soil and CANDE (B.M.) soil have the lowest earth pressure values, but the difference between these and the other values is considered insignificant. Thus, the soil type and its level of compaction above the culvert have very little effect on the earth pressure distribution at the haunches.

C. Soil at the extreme ends

The site soil and the CANDE (B.M.) soil exhibited the greatest earth pressure intensity (approximately 50 psi at 200 kips compared to 30 psi for the next highest soil) as illustrated in Figure 14. Further more, the CANDE (B.M.) correlated well with the site soil. The three poorly-compacted CANDE test soils (SW61%, ML49%, and CL45%) all had essentially zero earth pressure at the haunches for the entire range of loading (40 to 200 KIPS). This would seem to indicate that the poorly-compacted soils at the extreme ends induced very little, if any, soil-structure interaction. This would cause the arch structure to act independently of the soil, or as a freestanding structure. The three well-compacted test soils (SW95%, ML95% and CL95%) cause earth pressures that are somewhere between those of the poorly-compacted test soils and those of the site and CANDE (B.M.) soils. The SW95% values are basically half of the corresponding site soil values. The ML95% and CL95% earth pressure values are approximately one fourth as high as those for the site soil.

D. Soil below the foundation

The ML49% (poorly-compacted silt) causes the highest earth pressure distribution at the haunches (ranging from 30 to 70 psi) as shown in Figure 15. The SW61% (poorly-compacted sand) exhibits the second highest earth pressure intensity, which range from 10 to 70 psi. The results for other soils are all clustered together (0 to 50 psi). This would seem to indicate that the more poorly-compacted soils below the foundation induce higher earth pressures at the haunches.

3. Settlement below the foundation

By changing only engineering properties of the soil below the foundation, the CL45% (poorly-compacted clay) soil caused the highest settlement of about 14" (see Figure 16). This would be considered an extremely high settlement. The ML49% (poorly-compacted silt) and the SW61% (poorly-compacted sand) have very similar values and the next highest settlement of 9" to 11". Conversely, the well-compacted soils had extremely low displacements when compared to the poorly-compacted soils. The CL95% (well-compacted clay) displayed only about a 1" settlement. The ML95% and SW95% (the well-compacted silt and sand, respectively) had almost negligible settlements of approximately 1/4".

Figure 16 shows the extreme importance of obtaining good compaction on the foundation soils to reduce settlement. The poorly-compacted soils had settlements ranging from 9" to 14", while the well-compacted soils had settlements of one inch (1") or less. Thus, the poorly-compacted soils would provide an unsatisfactory performance while the well-compacted soils would perform well. It is assumed that the soils in other locations (backfill, top of culvert, and at the extreme ends) have a negligible effect on the settlement below the foundation. Some limited computer analyses were performed which seemed to confirm this. In real life situations, the foundation soil would typically be undisturbed. The soil would only be poorly-compacted if it was fill material or if the native soil were soft or loose.

4. Net Displacements

Another important parameter that required detailed analysis was the characteristics of the net displacement. The net displacement is defined as the displacement of the structure (at a given applied load) minus the settlements below the foundation discussed in the previous section. Both of these values were established by varying the soil properties below the foundation. The net displacements are shown in Figure 17.

At smaller applied loads (up to 200 kips), the well-compacted soils perform reasonably well and reach maximum net displacements of just over 2 inches. At 200 kips, the CL45% reaches a maximum net displacement of about 3 inches; the SW61% reaches a value of just under 4 inches; and the ML49% reaches a value just under 7 inches. Thus, the soils exhibiting lower compaction, especially the ML49% perform poorly below the 200-kip load range. At the 250-kip load increment, the well-compacted soils exhibit net displacements ranging from 2.5 to 3.5 inches; the poorly-compacted soils range from 5 to 9 inches. From 250 to 350-kip load increments, the net displacements all increase significantly. In general, these results reveal that the well-compacted soils perform better; although at very high applied load increments the ML95%, CL95% and even SW61% seem to exhibit smaller net displacements than the SW95% soils.

V. LIMITING STRUCTURAL RESPONSE

1. Displacements

The displacement of the structure is plotted versus its unfolded length for 200-kip load increment in Figure 18. It is observed that the displacement is near zero at the haunches and reaches its maximum quantity of 1.9" at mid-span of the arch. Incidentally, this trend correlates very well with the actual results recorded during the field testing of the arch culvert structure in the previous full-scale load test.

2. Steel Tensile Stresses

The reinforcing steel's yield strength was obtained in the laboratory at 83,700 psi. Using this yield strength, a series of CANDE runs was performed to determine the corresponding applied load increment.

The modified CANDE output revealed that the maximum allowable outer cage steel stress (i.e., 83,700 psi) occurs at an applied load of 232 kips as illustrated in Figure 19. The spikes in Figure 19 indicate the locations at which the outer cage steel begins to yield. This maximum steel stress takes place at a location midway between the haunches and mid-span on the outside face of the arch structure. For the inner cage steel, the maximum allowable steel stress occurs under an applied load increment of 239 kips at mid-span on the inside face of the structure (see Figure 20). The single spike in Figure 20 designates the point at which the inner cage steel begins to yield. It also specifies the location of the applied concentrated load.

3. Concrete Compressive Stresses

The concrete's compressive strength was obtained in the laboratory at 7,175 psi. Using the compressive strength of 7,175 psi, a series of CANDE runs was performed to determine the corresponding applied load increment.

The maximum allowable concrete compressive stress of 7,175 psi occurs at an applied load of 250 kips (see Figure 21). This maximum stress takes place at a location midway between the haunches and mid-span of the structure. A slightly lower stress is observed at mid-span. The spikes that appear in Figure 21 reveal the locations of the concentrated loads and the points at which crushing of the concrete commences.

The structural response was evaluated by plotting the thrusts, moments, and normal pressures for the unfolded length based on the steel tensile stress and concrete compressive stress as established above. The plots are included in Appendix G of this manuscript. A brief description of each figure is provided in the following sections.

4. Thrusts

Thrusts were computed and plotted versus the unfolded length of the structure for applied load increments of 200 kips, 232 kips, 239 kips, and 250 kips, respectively. The same trend is observed for the various load increments; i.e., with the lowest thrust magnitude at the foundation level and reaching the greatest magnitude at the haunches. For instance the maximum thrust intensities are 3,700 lb/in, 4,150 lb/in, 4,250 lb/in, and 4,500 lb/in at 200-kip, 232-kip, 239-kip, and 250-kip load increments, respectively. There seems to be a significant jump in the thrust magnitudes from the 239-kip to 250-kip load increments. Figure 22 exhibits the variation in thrust values as a function of unfolded length at an applied load of 239 kips. Yielding of reinforcing steel appears to occur at the 239-kip load since the thrusts increase sharply beyond this point.

5. Moments

Moments were computed and plotted versus the unfolded length of the structure for applied load increments of 200, 232, 239, and 250 kip. All of the plots follow essentially the same trend; i.e., zero values at the supports and maximum negative quantities at the haunches and maximum positive moments at the mid-span (see Figure 23). The magnitudes of maximum moments for the given load increments are listed in the table below.

Table 2. Maximum negative and positive moments for various loading applications.

Applied Load Increment (kips)	Negative Moment (in-lb/in)	Positive Moment (in-lb/in)
200	100,000	83,000
232	108,000	92,000
239	110,000	95,000
250	112,000	100,000

There doesn't seem to be any obvious change in the pattern of the moment values for the range of applied load increments considered herein, which would indicate yielding. In the next section of this report, entitled "Ultimate Load Testing" the effect of even greater magnitude applied load increments on the moment values will be investigated.

6. Normal Soil Pressures

Normal soil pressures on the structure were computed and plotted versus the unfolded length for applied load increments of 85, 200, 232, 239, and 250 kips, respectively. A typical curve, representing the normal soil pressure as a function of the structure's unfolded length, appears in Figure 24 for 239-kip load increment. It is apparent from this figure that the normal soil pressure reaches its maximum intensity near the haunches. The spikes on the sketch appear to be at the locations of the concentrated loads. Table 3 below lists the various intensities of normal soil pressures for the above load increments.

Table 3. The maximum normal soil pressures for the given applied load increments.

Applied Load Increments (kips)	Normal Soil Pressures (psi)
85	-27.5
200	-62.5
232	-71.5
239	-73.5
250	-77.0

There is no obvious change in the pattern of the normal soil pressure throughout the range of these applied load increments, which would indicate yielding. The normal pressures did seem to increase somewhat more rapidly between the 239 kips and 250 kips load increments. This may reveal that the yielding might have occurred at about 239 kips.

VI. ULTIMATE LOAD TESTING

The CANDE finite-element computer program was utilized to estimate the ultimate load carrying capacity of the arch culvert structure with respect to:

1) Displacement at various locations on the structure,
2) Soil pressures at the top and bottom of the structure,
3) Moments along the unfolded length of the structure, and
4) Thrusts as a function of the unfolded length.

The applied loads were incrementally increased up to about 400 kips and structural response were evaluated and the results were plotted versus the load values. Typically, the above structural responses followed essentially similar trend; i.e., they increased to a maximum quantity and then deceased dramatically. The point at which dramatic change in structural response occurred was considered to be the ultimate failure.

1. Displacement at the Center (Location No. 4)

The mid-span displacement obtained from the CANDE computer program agree very well with the actual displacement monitored during the full-scale live load test up to 200 kips, which was the limit of the hydraulic jack's capacity. Beyond the applied load of 200 kips, the displacements computed by the CANDE continue to increase more rapidly. From 340 to 360 kips, the displacement increases greatly from about 7" to 12" (see Figure 25). Beyond the 360-kip load increment, the displacement decreases dramatically down to approximately 6.5". This indicates that failure has occurred at an applied load around 340 to 360 kips. It is important to realize that the CANDE finite-element computer program was developed based on small-displacement theory. Thus, the results in the large-displacement range are inconsequential.

2. Displacement Near the Bottom of Culvert Walls (Locations No. 1 & 7)

The displacements at locations 1 & 7 from the CANDE program agree very well with the actual field displacements up to 200-kip load increment (see Figure 26). Beyond the 240-kip load increment, the displacements increase more rapidly, especially from 340 to 360 kips (from 0.18 inch to 0.26 inch). At about 380 to 400 kips, the displacement drops back down to approximately 0.20 inch. Thus, it can be concluded that the structural failure must have occurred around 34 kips, just as it did for the displacement at the center.

3. Displacements Near the Haunches (Locations No. 2 & 6)

The displacements at the haunches, obtained from the CANDE program, agree reasonably well with the actual field data up to 200-kip load increment. Beyond the 240-kip load increment, however, the displacements computed by CANDE increase more rapidly. From 340 kips to 360 kips, the displacements increase from 0.8 inch to 1.2 inches (see Figure 27). At about 380 to 400 kips, the displacements decrease back to the 0.80-inch range. Thus, it appears that the failure due to displacement must have occurred at an applied load of about 340 kips.

4. Displacements Midway Between Mid-Span and the Haunches (Locations No. 3 & 5)

The displacements at locations 3 and 5 obtained from the CANDE program correlate very well with the actual field data up to 200-kip load increment as shown in Figure 28. From the 200-kip to 320-kip load increments, the displacements decrease from 0.25 inch down to about 0.03 inch. There is no apparent reason for this reduction in displacement. It may be due to the stiffness of haunches, since the thickness of the haunches are greater than other segments of the culvert. Beyond the 320-kip load increment, the displacement rises quickly up to 0.30 inch at 340 kips, 1.0 inch at 350 kips, and a high of 1.2 inches at 360 kips. Beyond 360-kip load increment, it drops back down to 0.40 inch. This displacement failure also occurred at an applied load increment between 340 kips and 350 kips. Evidently, the ultimate value of 350 kips is the maximum load the structure can withstand with respect to displacement.

5. Earth Pressure at the Bottom

The results of the CANDE program for soil pressure distribution match the field data only up to 80-kip load increment as depicted in Figure 29. Beyond the 80-kip load increment, up to 200 kips, the CANDE program overestimates the soil pressure by 30% to 100%. It should be noted that only the earth pressure cell on the east side of the unit was successfully monitored.

The comparable earth pressure cell on the west side malfunctioned during the live load testing. Above about the 240-kip load increment, the pressure computed from the CANDE program starts increasing more rapidly; it increases from 45 psi at 340 kips of applied load up to about 60 psi at 360 kips. At load increments around 380 kip to 400 kips, the soil pressure dropped back down to about 45 psi. Accordingly, the structure reached its ultimate load carrying capacity at a corresponding earth pressure on the bottom of the sidewall at an applied load between 340 kips to 360 kips. This is the same range as the values obtained based on the displacement failure criterion discussed in the previous sections.

6. <u>Earth Pressure at the Top</u>

The earth pressure distribution computed by the CANDE program correlates very well with the field data up to 200-kip load increment (i.e., the upper limit of the load testing). Above about 240 kips, the soil pressure computed by CANDE starts increasing more rapidly; it reaches 140 psi at 340 kips, and up to 200 psi at 360 kips applied load (see Figure 30). The soil pressure drops back down to about 145 psi at load increments ranging from 380 to 400 kips.

Thus, the structural failure corresponds to a soil pressure on the top at an applied load between 340 kips to 350 kips. It should be noted that the pressures at the top were much higher than the pressures at the bottom because the live loads (representing vehicular loading) have a much greater effect on the top of the sidewalls than on the bottom of the sidewalls.

7. <u>Moments</u>

The moments on the structure were calculated using the CANDE program at applied loads of 240 kips, 280 kips, 320 kips, and 360 kips, respectively. The moment diagrams were then plotted for each of these four applied loads. Only moment diagrams for the 320-kip and 360-kip load increments are shown in Figures 31 and 32. The moment diagrams for the 240-kip, 280-kip, and 320-kip load increments appeared to follow the same trend (for instance, see Figure 31 for the moment plot of 320-kip load increment). The moment diagram corresponding to 360-kip load increment, however, revealed a considerably different trend (see Figure 32). This latter plot shows a combination of positive and negative moments in the leg of the culvert. Also, the magnitude of maximum negative moment dropped considerably from 126,370 in-lb/in at the 320-kip load increment to 91,700 in-lb/in at the 360-kip load increment. The moment value of 91,700 in-lb/in at the 360-kip load increment is even lower than the moment value of 110,400 in-lb/in for the 240-kip load increment. Thus, the structural failure corresponds to high moments at an applied load between 330 kips to 350 kips.

In summary, the results of the computer analysis concerning the soil-structure interaction study of the reference Precast concrete arch culvert furnishes the following insights. The values of displacements at various locations on the structure, soil pressures, and moments typically increased with increasing applied loads up to a maximum limit of 350 kips. The only notable exception to the constant increase was the displacement at locations number 3 and 5, which decreased from 200 kips to 320 kips. This could be the subject of further study for a future project. All of the values of displacements, soil pressures, and moments had the largest incremental increase between 340 kips and 35 kips, and then dropped dramatically beyond this point. Thus, it can be inferred that the structure failed at an applied load between 340 kips and 350 kips. This is an impressive value of 13 times greater than the design load of 26 kips.

VII. CONCLUSIONS

The parametric studies of the arch culvert structures entailed the evaluation of the mid-span displacement, earth pressure distribution, settlements below the foundation, and net displacements below the foundation by using the CANDE finite-element computer program. Varying the soil types below the foundation (especially the ML49% type soil) caused very high displacements at the center of the structure. The earth pressure distribution was influenced to some extent by altering the soil properties. In general, the well-compacted soils exhibited higher pressures at the haunches than the poorly-compacted soils (specifically with respect to backfill soil and soil at the extreme ends).

The ML95% and CL95% soil types below the foundation supports exhibited the lowest net displacements. The SW95% soil had similar net displacement as the above two soil types, but its values increased more dramatically at the 350-kip load increment. Among the poorly-compacted soils, the SW61% fared surprisingly well. The CL45% performed poorly (with regard to net displacements) at the higher loads, while the ML49% performed poorly for the entire range of applied loads.

The ultimate load carrying capacity of the culvert structure was also investigated based on the displacements at various locations, earth pressure distribution, bending moments, and thrusts, utilizing the CANDE finite-element computer program. First, the stresses at which yielding of reinforcing steel and crushing of concrete occurred were established in the laboratory. Then, a series of CANDE runs was conducted to determine the corresponding applied loads. It was found that the steel yields at an applied load increment from 230 to 240 kips, while the concrete begins crushing at an applied load of approximately 250 kips.

Once the above loads are reached (i.e., the loads at which the yielding of steel and crushing of the concrete take place), the structure begins to form plastic hinges and behaves as a three-hinged arch. The hinges are located near the haunches and at mid-span. Evidently, the structure is still stable and capable of sustaining additional loads prior to ultimate failure. Consequently, the applied loads were incrementally increased to gauge the structural response with respect to displacements, moments, and soil pressures. It was observed that as the applied load increased beyond the 250-kip increment, the values of displacements, moments, and earth pressures increased rapidly to a maximum level and then abruptly tapered off. The point at which sudden change of structural response took place, was considered to be the ultimate failure. Based on this methodology and the concept of soil-structure interaction, the ultimate load that arch culvert structure can withstand is approximately 340 kips. This is an impressive 13 times greater than the design load of 26 kips.

VIII. ACKNOWLEDGEMENTS

The present research project was partially sponsored by the Ohio Department of Transportation (ODOT). Financial support of ODOT is acknowledged. Thanks are extended to the CON/SPAN Bridge Systems for furnishing the shop drawings and other figures.

IX. REFERENCES

1. Zoghi, M., Predicting the Performance of A Long-Span Precast Concrete Arch Culvert, Final Report Submitted to the Ohio Department of Transportation (ODOT), Project No. 93438, January 1994.

2. Musser, S.C., CANDE-89 Culvert ANalysis and DEsign Program, User Manual, No. FHWA-RD-89-169, U.S. Department of Transportation, 1989.

3. Construction and Material Specifications, State of Ohio Department of Transportation, Columbus, Ohio, January 1, 1995.

4. AASHTO, "Recommended Practice for Classification of Soils and Soil-Aggregate Mixtures for Highway Construction," AASHTO Designation M 145-91, Standard Specifications for Transportation Materials and Methods of sampling and Testing, American Association of State Highway and Transportation Officials, Washington, DC, 1993.

5. Seed, R.B., Bray, J.D., and Thomas, D.C., "Analysis, Design, and Prototype Testing of a Smooth-Walled Box Culvert System," Transportation Research Record 1231, TRB, National Research Council, Washington, D.C., 1989, pp 1-13.

6. Katona, M.G., et al, "Structural Evaluation of New Concepts for Long-Span Culverts and Culvert Installations," Report FHWA-RD-79-115, U.S. Department of Transportation, 1979.

7. Selig, E.T., "Soil Parameters for Design of Buried Pipelines," ASCE Conference on Pipeline Infrastructure, June 1988.

8. CON/SPAN Bridge Systems Design Manual, Dayton, Ohio, 1996.

9. McGrath, T.J., Selig, E.T., and Beach, T.J., "Structural Behavior of Three-sided Arch Span Bridge," Transportation Research Record 1541, TRB National Research Council, Washington, D.C., 1996.

10. Katona, M.G., et al, CANDE – A Modern Approach for Structural Design and Analyses of Buried Culverts, FHWA-RD-77-5, U.S. Naval Civil Engineering Laboratory, 1977.

Appendices:

- Appendix A – Tables of Soil Properties
- Appendix B – CANDE Benchmark Soil Properties
- Appendix C – Culvert Schematic and Shop Drawings
- Appendix D – Culvert's Beam-Column Elements Assemblage and Finite-Element Mesh
- Appendix E – Output of CANDE Run for 200-kip Load Increment
- Appendix F – Soil Elements Representing Concrete Footings, Native Soil, Backfill Soil, and Cover Soil
- Appendix G – Figures Presenting the Parametric Studies

Appendix A

Tables of Soil Properties For Six CANDE Test Soils

Table 4 Soils Used in Property Tests

Soil Type	Classification USCS	Classification AASHTO	Consistency(%) Liquid Limit	Consistency(%) Plasticity Index	AASHTO T-99 Compaction Maximum Dry Density (pcf)	AASHTO T-99 Compaction Optimum Moisture (%)
Gravelly Sand	SW	A1	--	N.P.	138	7.4
Sandy Silt	ML	A4	20	4	119	12.1
Silty Clay	CL	A6	32	15	103	21.0

1 lb/cu ft = 0.016 Mg/m^3 = 0.157 kN/m^3

Table 5 Triaxial Test Parameters

Soil Type	% T-99	K	n	R_f	C (psi)	ϕ_o (deg)	$\Delta\phi$ (deg)
SW	95	950	0.60	0.70	0	48	8
	90	640	0.43	0.75	0	42	4
	85	450	0.35	0.80	0	38	2
	80	320	0.35	0.83	0	36	1
	61	54	0.85	0.90	0	29	0
ML	95	440	0.40	0.95	4	34	0
	90	200	0.26	0.89	3.5	32	0
	85	110	0.25	0.85	3	30	0
	80	75	0.25	0.80	2.5	28	0
	49	16	0.95	0.55	0	23	0
CL	95	120	0.45	1.00	9	15	4
	90	75	0.54	0.94	7	17	7
	85	50	0.60	0.90	6	18	8
	80	35	0.66	0.87	5	19	8.5
	45	16	0.95	0.75	0	23	11

1 psi = 6.9 kPa

Table 6 Hydrostatic Test Parameters

Soil Type	% T-99	Power Law Model Curve A K_b	Power Law Model Curve A m	Power Law Model Curve B K_b	Power Law Model Curve B m	Hyperbolic Model B_i/P_a	Hyperbolic Model ε_u
SW	95	250	0.80	250	0.0	74.8	0.02
	90					40.8	0.05
	85	90	1.02	130	0.10	12.7	0.08
	80					6.1	0.11
	61	35	1.59	35	0.82	1.7	0.23
ML	95	110	0.60	185	0.00	48.3	0.06
	90					18.4	0.10
	85	35	0.49	45	0.25	9.5	0.14
	80					5.1	0.19
	49	15	1.40	15	0.94	1.3	0.43
CL	95	50	0.60	80	0.20	21.2	0.13
	90					10.2	0.17
	85	25	1.05	30	0.55	5.2	0.21
	80					3.5	0.25
	45	15	1.77	15	1.02	0.7	0.55

Table 7 Placement Soil Parameters

Soil Typé	% T-99	Coefficient K_o	Wet Unit Weight γ_m (lb/cu ft)
SW	95	1.3	141
	90	1.1	134
	85	0.9	126
	80	0.8	119
	61	0.5	91
ML	95	1.2	127
	90	0.9	120
	85	0.8	114
	80	0.7	107
	49	0.5	66
CL	95	0.8	119
	90	0.6	112
	85	0.5	106
	80	0.4	100
	45	0.3	56

---

1 lb/cu ft = 0.016 Mg/m^3 = 0.157 kN/m^3

Appendix B

CANDE Benchmark Soil Properties

APPENDIX B

Table 8. The CANDE Benchmark Soil Properties

SOIL PROPERTIES

BACKFILL (SELIG MODEL)

SOIL NO:13	UNIT WT.	K	N	R_f	B_i/P_a	e_u	c	Φ	ΔΦ	K_o
VALUE RECOMEN.	125	408	0	0	340	100000	100	50	0	1
VALUE CHANGED		450		0.7	300					

BELOW FOUNDATION & EXTREME ENDS (SELIG MODEL)

SOIL NO:19	UNIT WT.	K	N	R_f	B_i/P_a	e_u	c	Φ	ΔΦ	K_o
VALUE RECOMEN.	145	6800	0	0.0	3800	100000	100	50	0	1
VALUE CHANGED				0.7						

Appendix C

Culvert Schematic and Shop Drawings

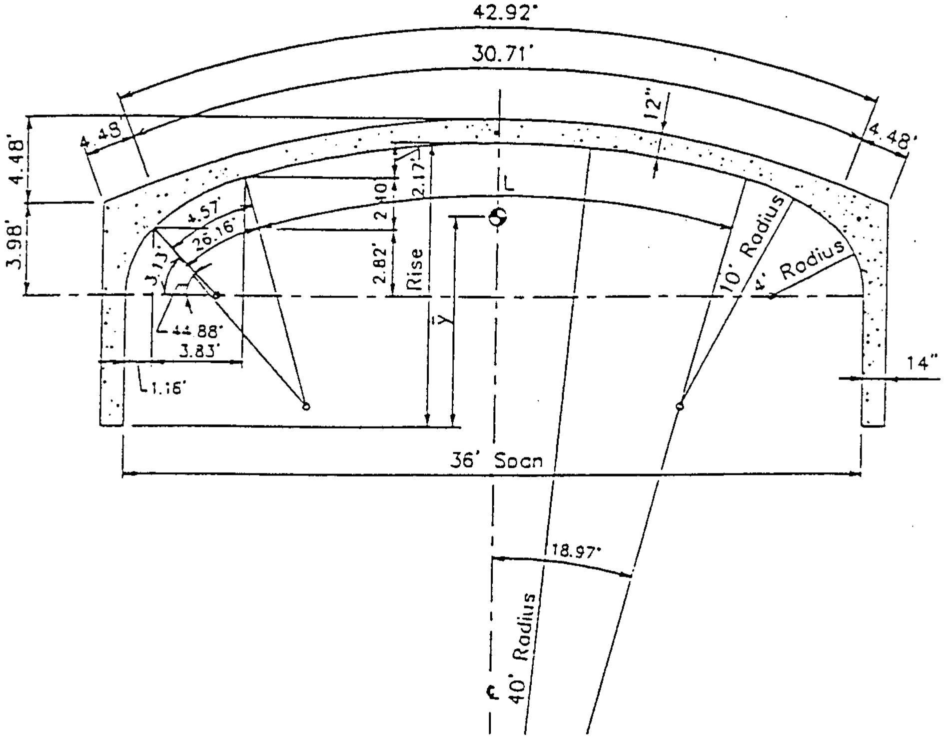

Figure No. 1

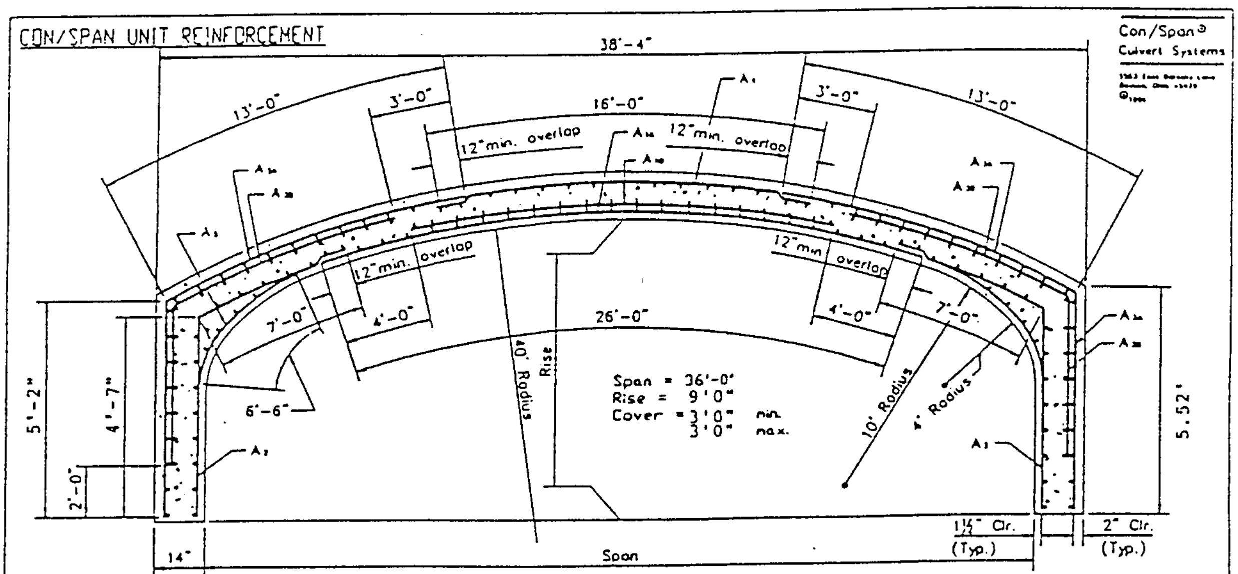

Sheet no.	Circumferential Area Req'd (in²/ft)	Longitudinal Area Req'd (in²/ft)	Mesh Size	Length (ft) **	Circumferential Area Supl'd (in²/ft)	Longitudinal Area Supl'd (in²/ft)
1	A1a = 0.72	0.13	2x8 - W12.0	26'-0"	0.72	0.13
2	A1b = .60	0.0	2x8 - W10.0	18'-0"	0.60	0.0
3	A2 = 0.48	0.13	2x8 - W8.0	11'-7"	0.48	0.13
4	A3a = 0.60	0.13	2x8 - W10.0	18'-2"	0.50	0.13
5	A3b = 0.60	0.0	2x8 - W10.0	13'-2"	0.60	0.0
6	A4 = 0.48	0.13	2x8 - W8.0	16'-0"	0.48	0.13
7	A5 = 0.48	0.13	2x8 - W8.0	6'-6"	0.48	0.13

Design Loading: HS25

*f'c = 6000 p.s.i.

** All splices should be measured from the first cross wire.

Producer: ESSROC - DELAWARE

Project: #2404 GAY ROAD BRIDGE MONTGOMERY COUNTY

Date: | Appr'd By

Con/Span is a patented system and the furnishing of this drawing does not constitute an express or implied license

Figure No. 2

Appendix D

Typical Assemblage of Culvert Beam-Column Elements And Finite-Element Mesh

Figure 3

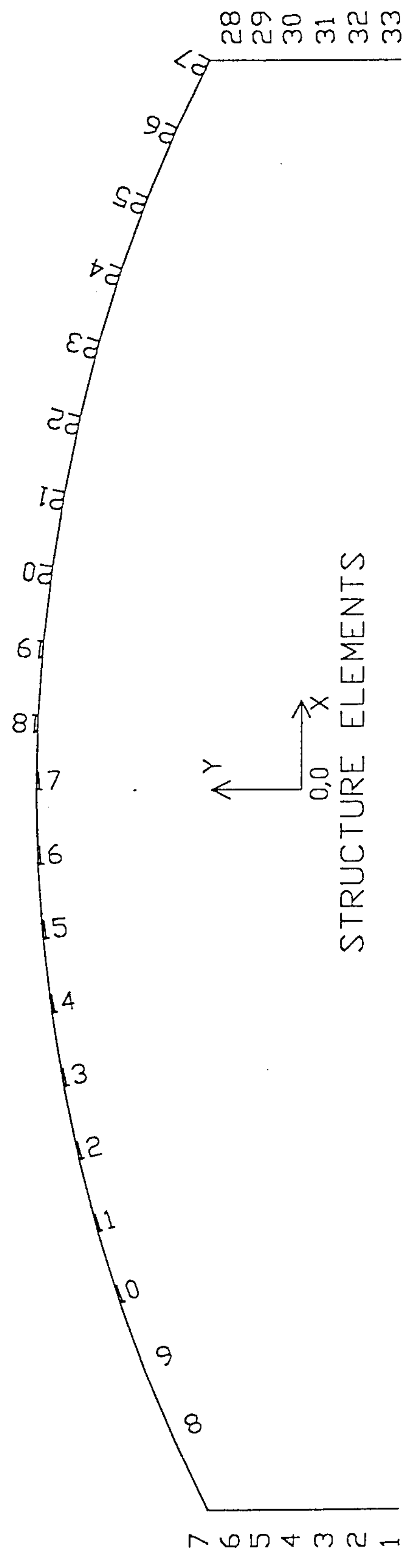
STRUCTURE ELEMENTS
0,0
X
Y
1
2
3
4
5
6
7
8
9
10
11
12
13
14
15
16
17
18
19
20
21
22
23
24
25
26
27
28
29
30
31
32
33

Figure 4

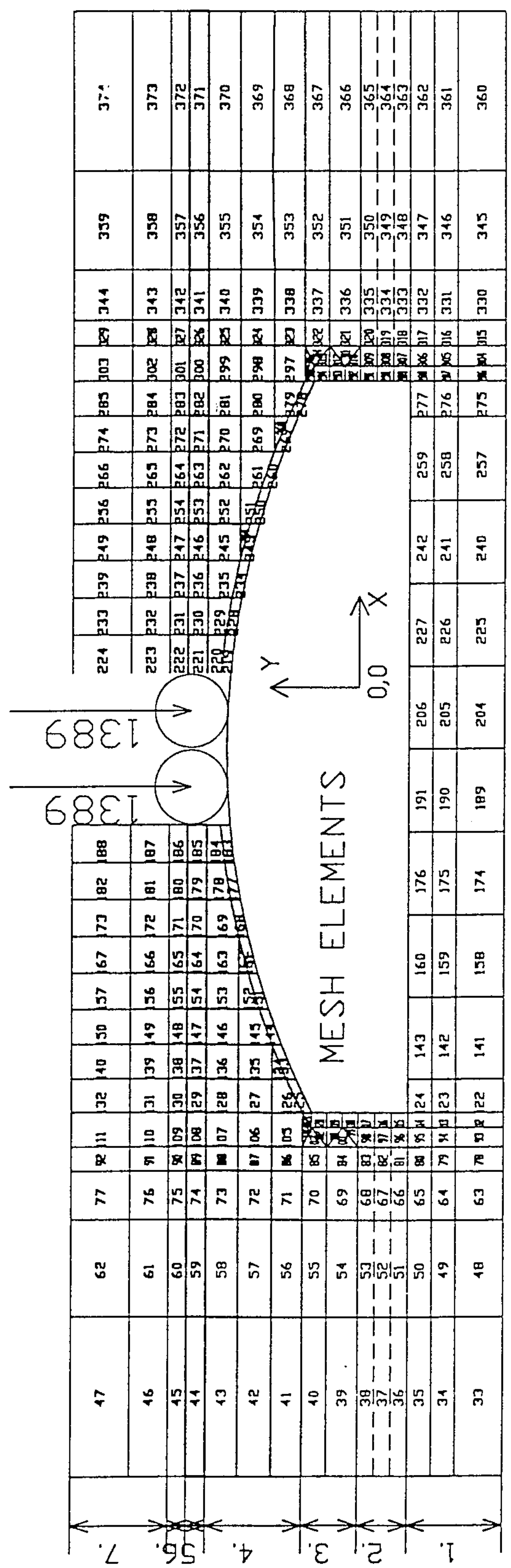

Figure 5

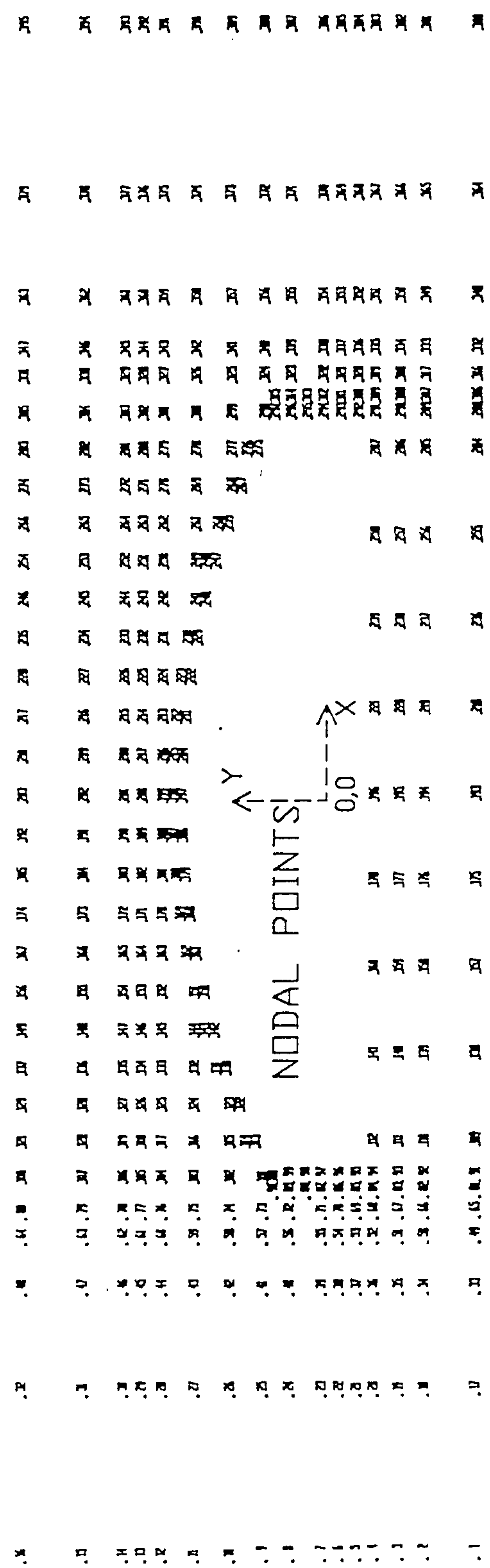

Appendix E

Output of CANDE Run for 200-kip Load Increment

Figure 6

OUTPUT OF CANDE FILE FOR 200 KIPS LOAD

(C)ULVERT (AN)ALYSIS AND (DE)SIGN II
I

VERSION 1.0
MARCH 1990

modified by LOCKWOOD, JONES & BEALS
DATED 01/01/92

*** PROBLEM NUMBER 1 ***

CON/SPAN ARCH CULVERT (36'S 9'R 2'C, HS25, FL, #2404)

EXECUTION MODE .....ANAL

SOLUTION LEVEL .....F.E.USER

CULVERT TYPE ...... CONCRETE

***NEGATIVE PIPE DIAMETER IMPLIES NEW CANDE OPTION FOR VARIABLE CONCRETE THICKNESS. ***

***OPTION IS RESTRICTED TO ANALYSIS ONLY WITH LEVEL 2-BOX, OR LEVEL 3. ***

PIPE PROPERTIES ARE AS FOLLOWS ...
(UNITS ARE INCH-POUND SYSTEM)

NOMINAL PIPE DIAMETER .... -
1.0000

CONCRETE COMPRESSIVE STRENGTH .....
7175.0000

CONCRETE ELASTIC MODULUS ....
4828206.0000

CONCRETE POISSON RATIO ....
0.1700

DENSITY OF PIPE (PCF).............. 150.0000

STEEL YIELD STRENGTH ....
83700.0000

STEEL ELASTIC MODULUS ....
29000000.0000

STEEL POISSON RATIO 0.3000

NONLINEAR CODE (1,2,OR 3) 3

CONC. CRACKING STRAIN (1,2,3) .....
0.000130

CONC. YIELDING STRAIN (2,3) ....
0.000722

CONC. CRUSHING STRAIN (2,3) ....
0.002000

STEEL YIELDING STRAIN (3) ....
0.002626

* * BEGIN PREP OF FINITE ELEMENT INPUT * *

THE DATA TO BE RUN IS ENTITLED

CON/SPAN ARCH CULVRERT

NUMBER OF CONSTRUCTION INCREMENTS——
9

PRINT CONTROL FOR PREP OUTPUT——— 4

INPUT DATA CHECK——————— 0

PLOT TAPE GENERATION—————— 1

ENTIRE FINITE ELEMENT RESULTS OUTPUT— 0

THE NUMBER OF NODES IS—————— 395

THE NUMBER OF ELEMENTS IS————— 374

THE NUMBER OF BOUNDARY CONDITIONS IS—
57

M, S, T AT ELEM. END CONTROL IS——— 0

* * * BOUNDARY CONDITIONS * * *
(FORCES = LBS; DISPLACEMENTS = INCHES; ROTATIONS = DEGREES)

BOUNDARY LOAD X-FORCE OR Y-FORCE OR X-Y ROTATION BEAM ROTATIONAL
NODE STEP X-DISPLACEMENT Y-DISPLACEMENT BOUNDARY CONDITIONS

2 1 D = 0.0000E+00 F = 0.0000E+00
0.0000E+00 D
3 1 D = 0.0000E+00 F = 0.0000E+00
0.0000E+00 D
4 1 D = 0.0000E+00 F = 0.0000E+00
0.0000E+00 D
5 2 D = 0.0000E+00 F = 0.0000E+00
0.0000E+00 D
6 2 D = 0.0000E+00 F = 0.0000E+00
0.0000E+00 D
7 2 D = 0.0000E+00 F = 0.0000E+00
0.0000E+00 D
8 3 D = 0.0000E+00 F = 0.0000E+00
0.0000E+00 D

Appendix F

Soil Elements Representing:

- Concrete Footings
- Native Soil (Below Foundation)
- Backfill Soil
- Cover Soil

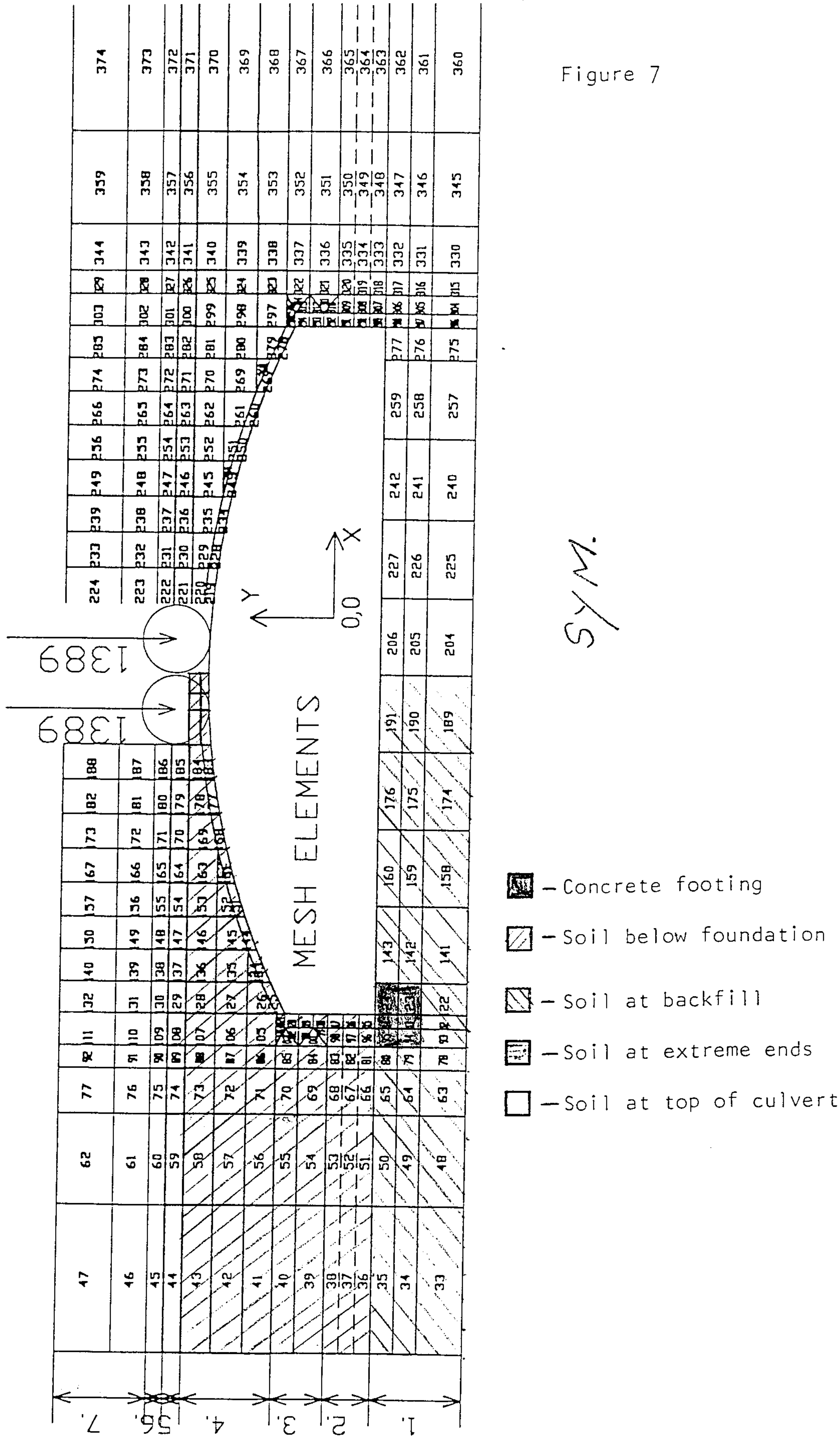
MESH ELEMENTS
SYM.
1389
1389
Y
X
0,0
– Concrete footing
– Soil below foundation
– Soil at backfill
– Soil at extreme ends
– Soil at top of culvert

Figure 7

Appendix G

Figures Presenting the Parametric Studies

Figure 8

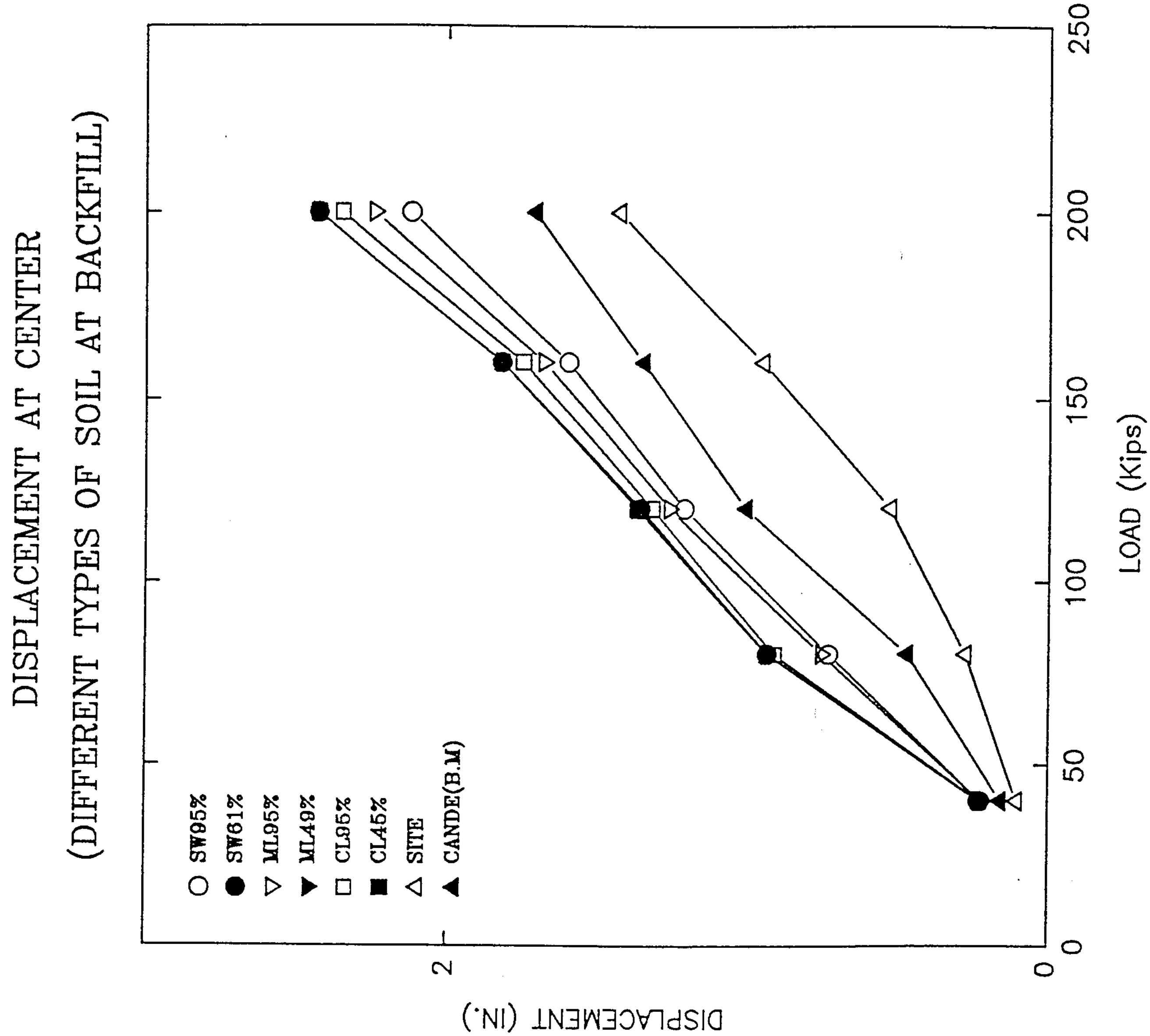
DISPLACEMENT AT CENTER
(DIFFERENT TYPES OF SOIL AT BACKFILL)
SW95%
SW61%
ML95%
ML49%
CL95%
CL45%
SITE
CANDE(B.M)
DISPLACEMENT (IN.)
2
0
LOAD (Kips)
0
50
100
150
200
250

Figure 9

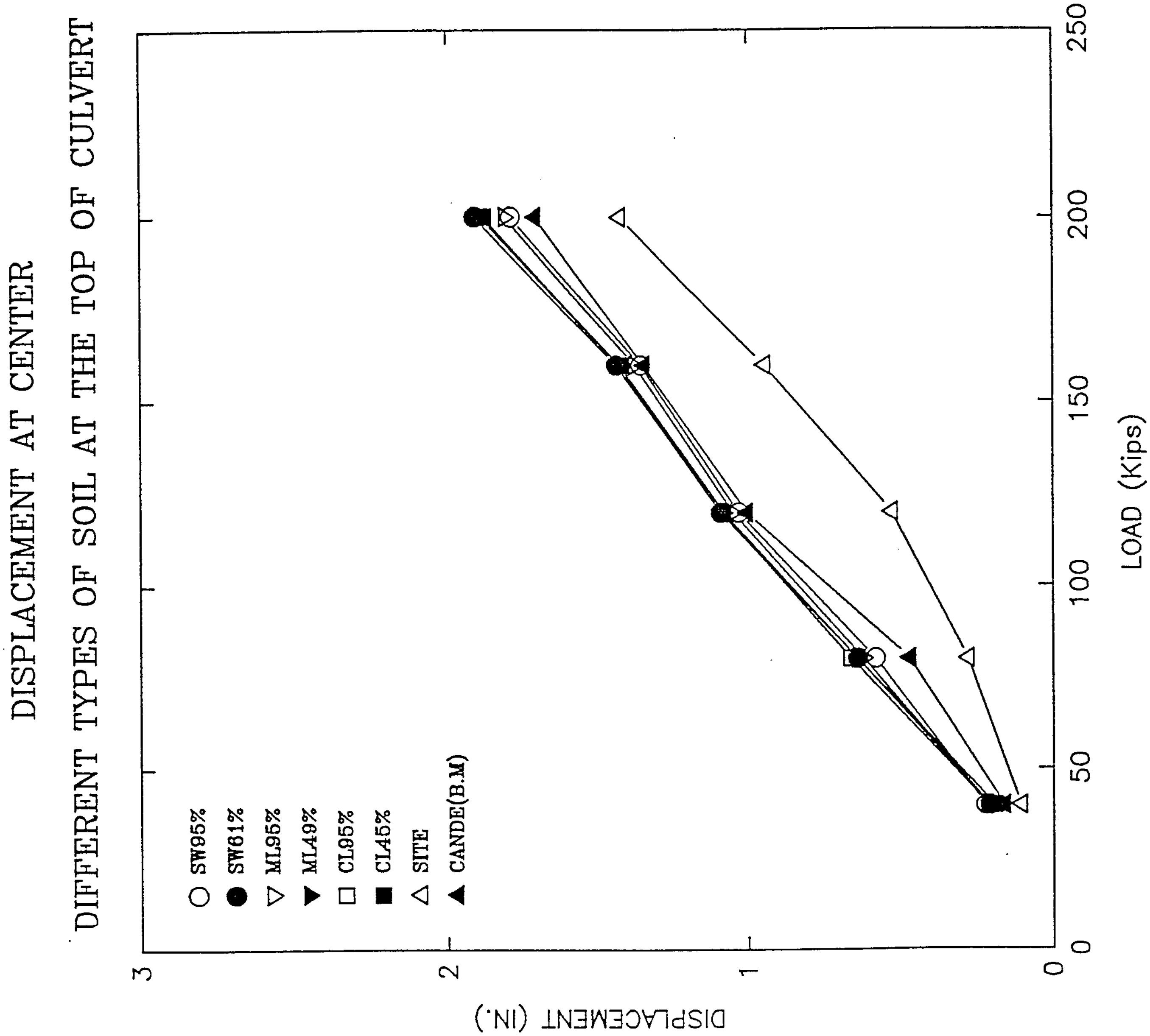
DISPLACEMENT AT CENTER
DIFFERENT TYPES OF SOIL AT THE TOP OF CULVERT
SW95%
SW61%
ML95%
ML49%
CL95%
CL45%
SITE
CANDE(B.M)
DISPLACEMENT (IN.)
LOAD (Kips)
0
1
2
3
0
50
100
150
200
250

Figure 10

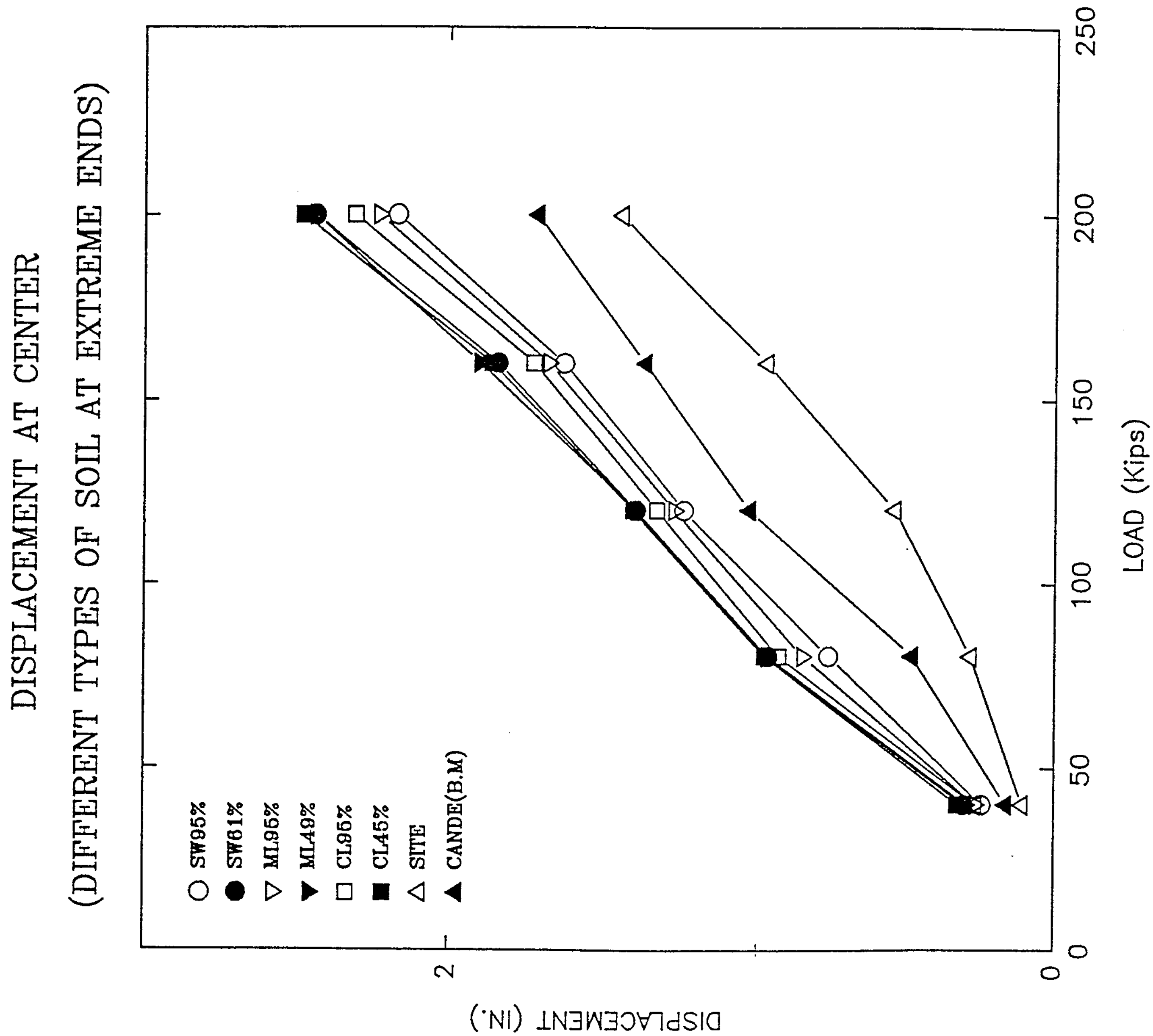
DISPLACEMENT AT CENTER
(DIFFERENT TYPES OF SOIL AT EXTREME ENDS)
SW95%
SW61%
ML95%
ML49%
CL95%
CL45%
SITE
CANDE(B.M)
DISPLACEMENT (IN.)
0
2
LOAD (Kips)
0
50
100
150
200
250

Figure 11

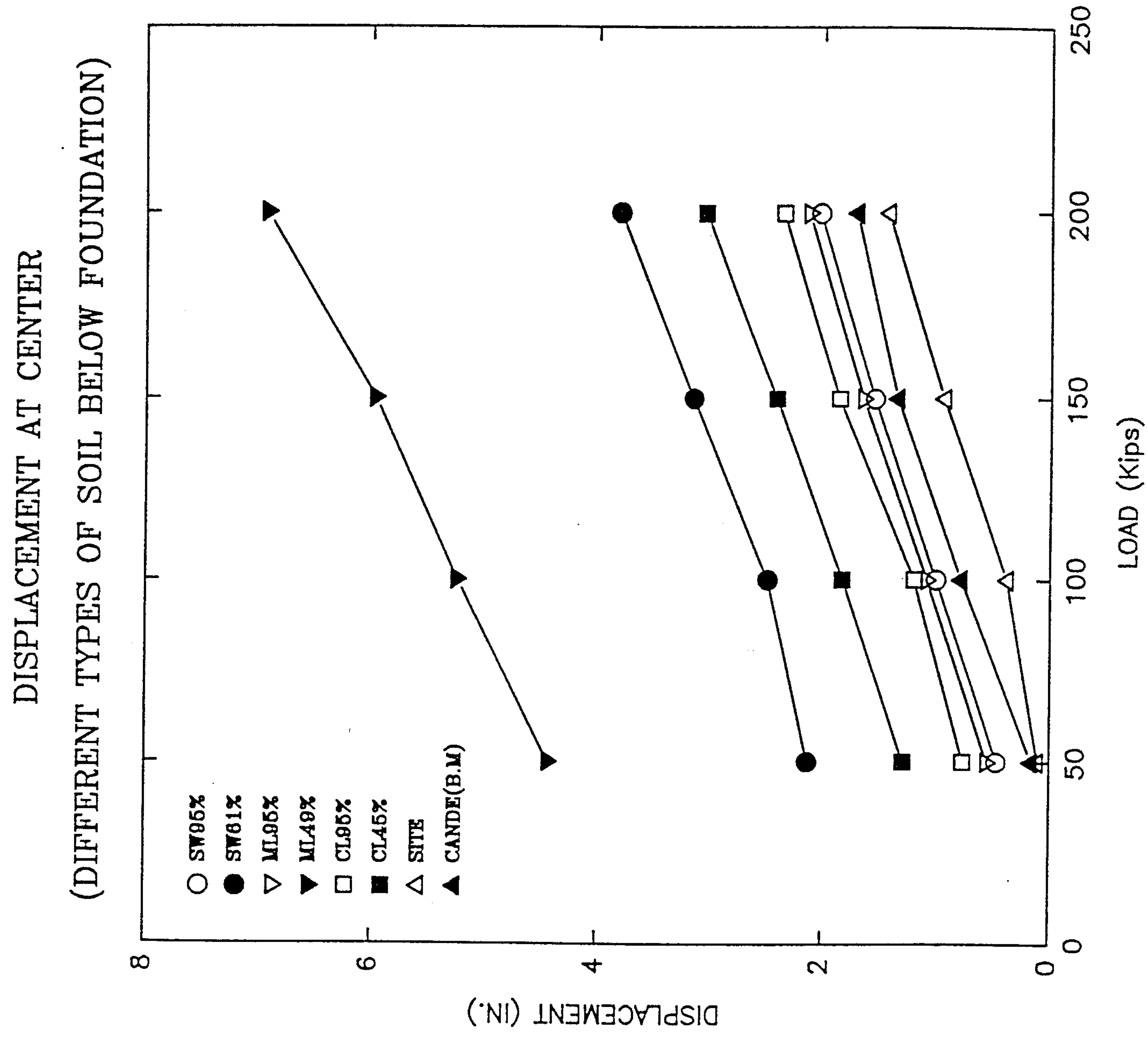
DISPLACEMENT AT CENTER
(DIFFERENT TYPES OF SOIL BELOW FOUNDATION)
SW95%
SW61%
ML95%
ML49%
CL95%
CL45%
SITE
CANDE(B.M)
DISPLACEMENT (IN.)
0
2
4
6
8
LOAD (Kips)
0
50
100
150
200
250

Figure 12

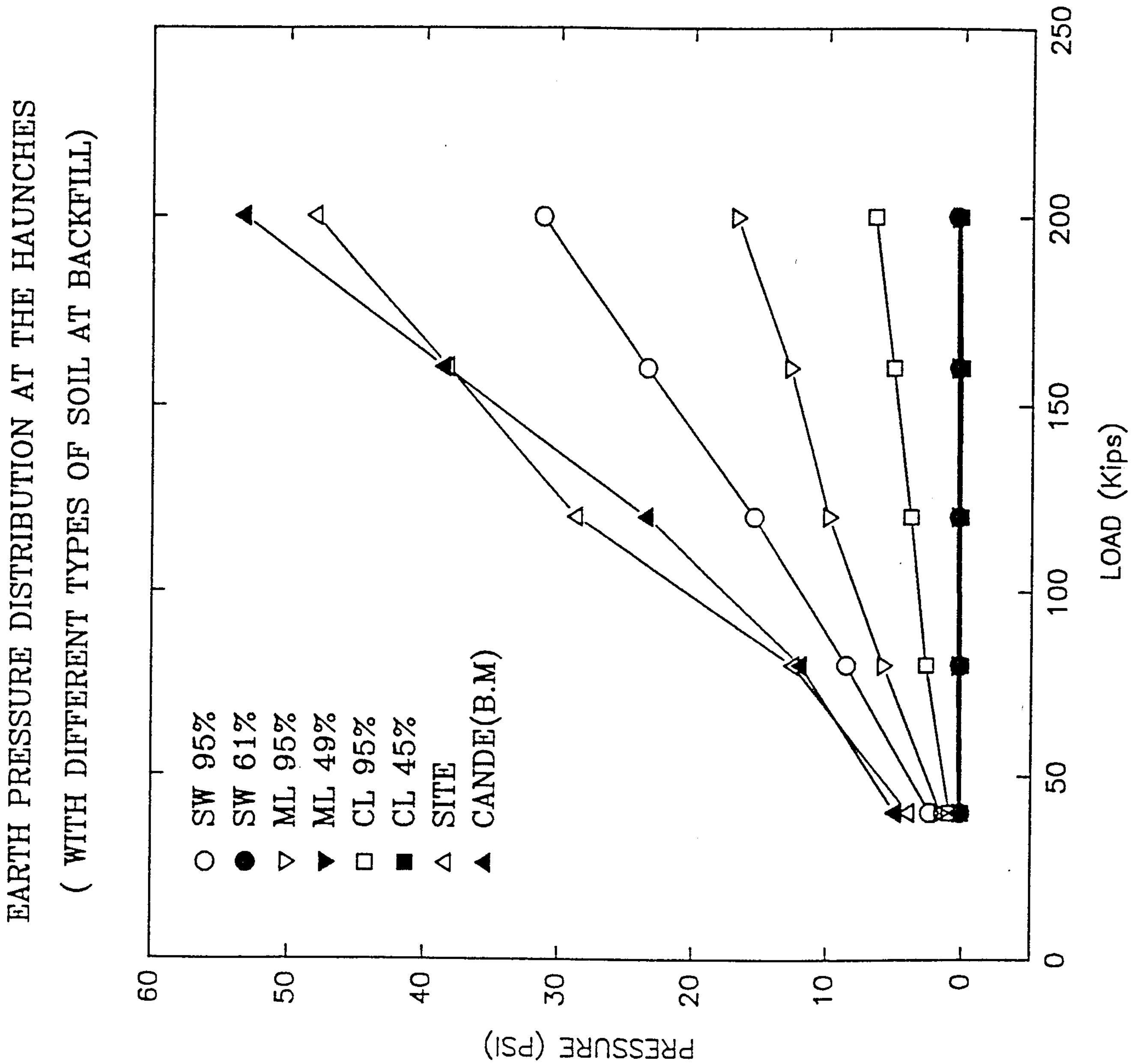
EARTH PRESSURE DISTRIBUTION AT THE HAUNCHES
(WITH DIFFERENT TYPES OF SOIL AT BACKFILL)
SW 95%
SW 61%
ML 95%
ML 49%
CL 95%
CL 45%
SITE
CANDE(B.M)
PRESSURE (PSI)
0
10
20
30
40
50
60
LOAD (Kips)
0
50
100
150
200
250

Figure 13

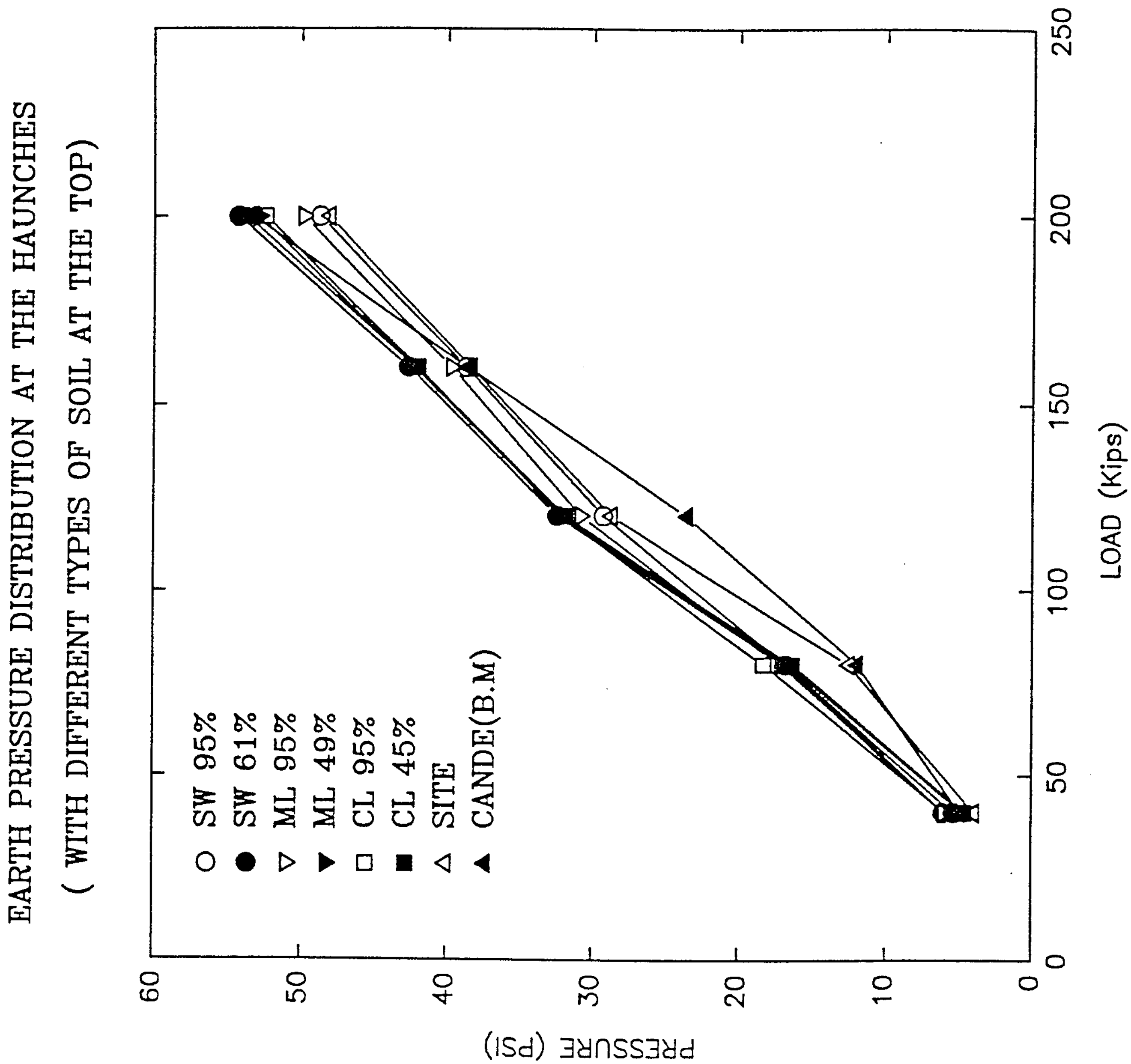
EARTH PRESSURE DISTRIBUTION AT THE HAUNCHES
(WITH DIFFERENT TYPES OF SOIL AT THE TOP)
SW 95%
SW 61%
ML 95%
ML 49%
CL 95%
CL 45%
SITE
CANDE(B.M)
PRESSURE (PSI)
LOAD (Kips)
0
10
20
30
40
50
60
0
50
100
150
200
250

Figure 14

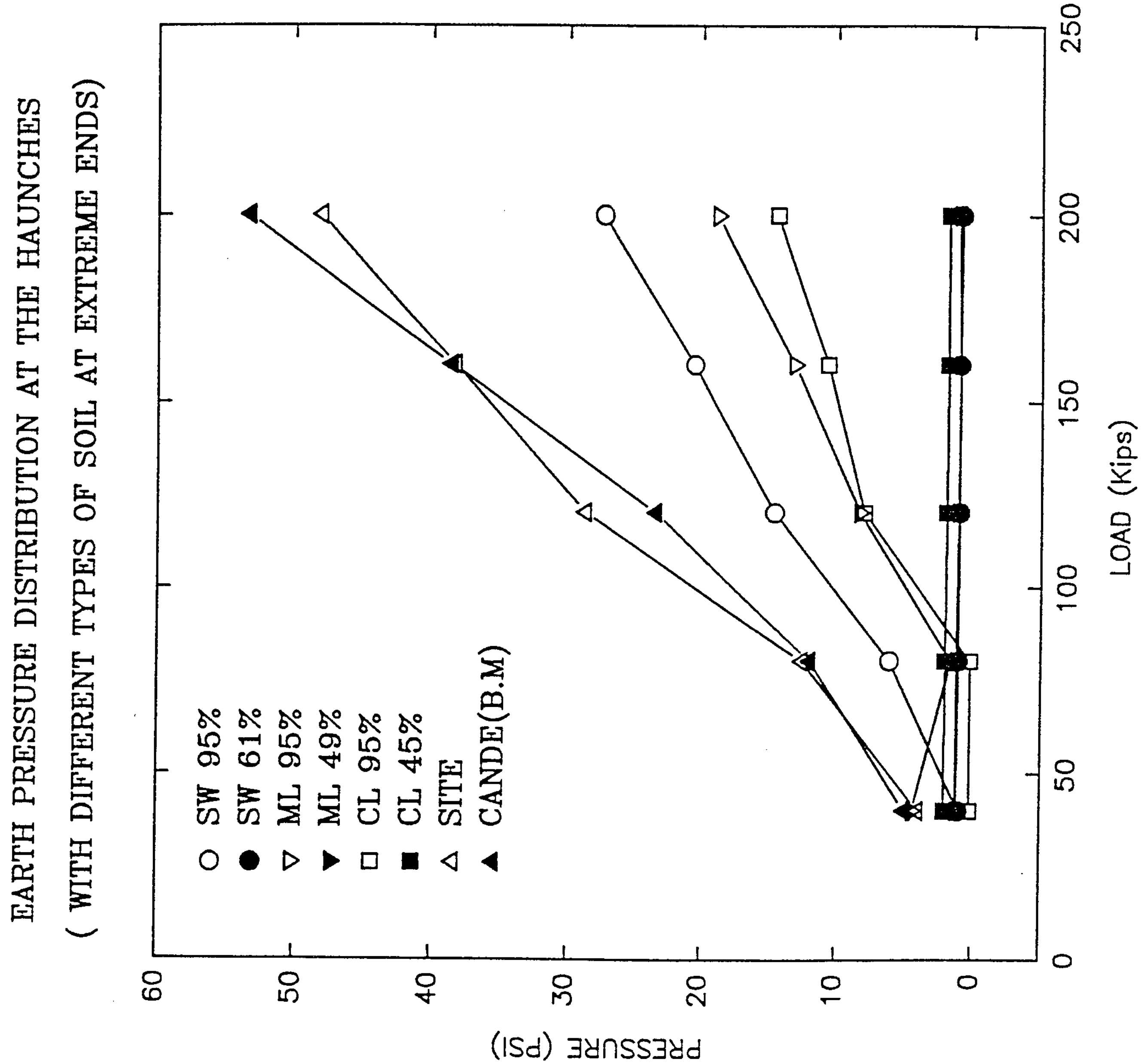
EARTH PRESSURE DISTRIBUTION AT THE HAUNCHES
(WITH DIFFERENT TYPES OF SOIL AT EXTREME ENDS)
SW 95%
SW 61%
ML 95%
ML 49%
CL 95%
CL 45%
SITE
CANDE(B.M)
PRESSURE (PSI)
LOAD (Kips)
0
10
20
30
40
50
60
0
50
100
150
200
250

Figure 15

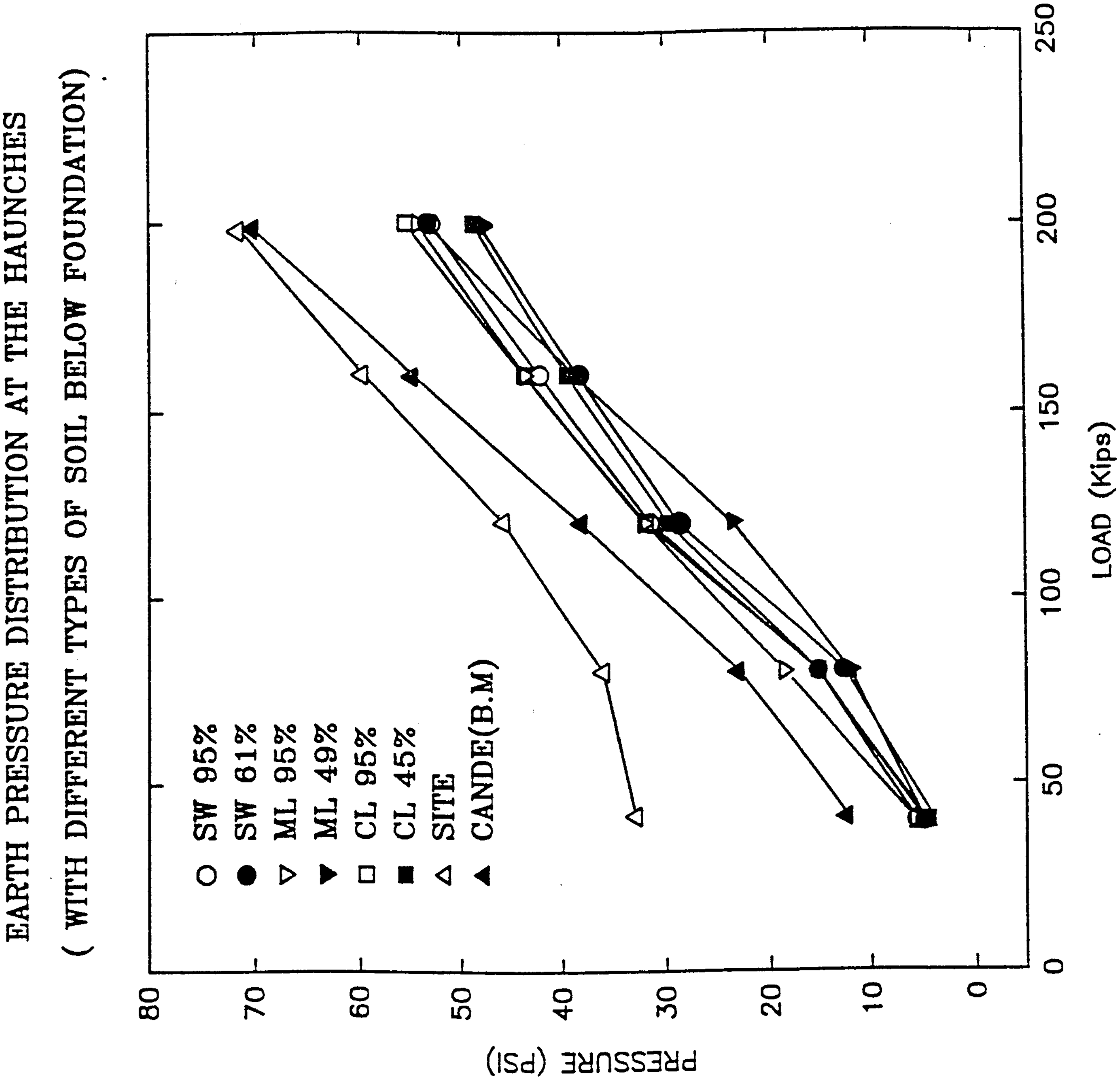
EARTH PRESSURE DISTRIBUTION AT THE HAUNCHES
(WITH DIFFERENT TYPES OF SOIL BELOW FOUNDATION)
SW 95%
SW 61%
ML 95%
ML 49%
CL 95%
CL 45%
SITE
CANDE(B.M)
PRESSURE (PSI)
0
10
20
30
40
50
60
70
80
LOAD (Kips)
0
50
100
150
200
250

Figure 16

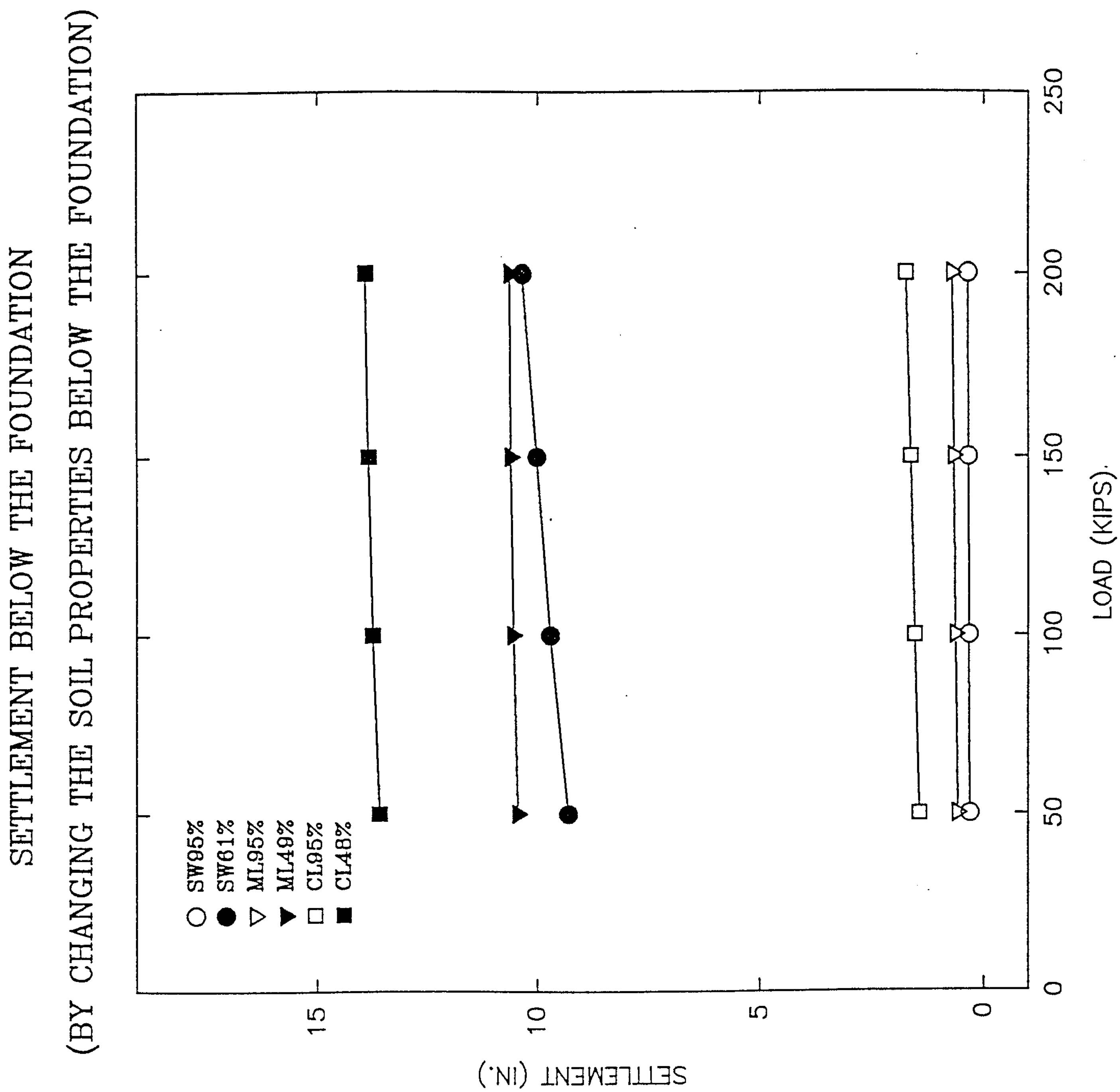
SETTLEMENT BELOW THE FOUNDATION
(BY CHANGING THE SOIL PROPERTIES BELOW THE FOUNDATION)
SW95%
SW61%
ML95%
ML49%
CL95%
CL48%
SETTLEMENT (IN.)
0
5
10
15
LOAD (KIPS)
0
50
100
150
200
250

Figure 17

NET DISPLACEMENTS

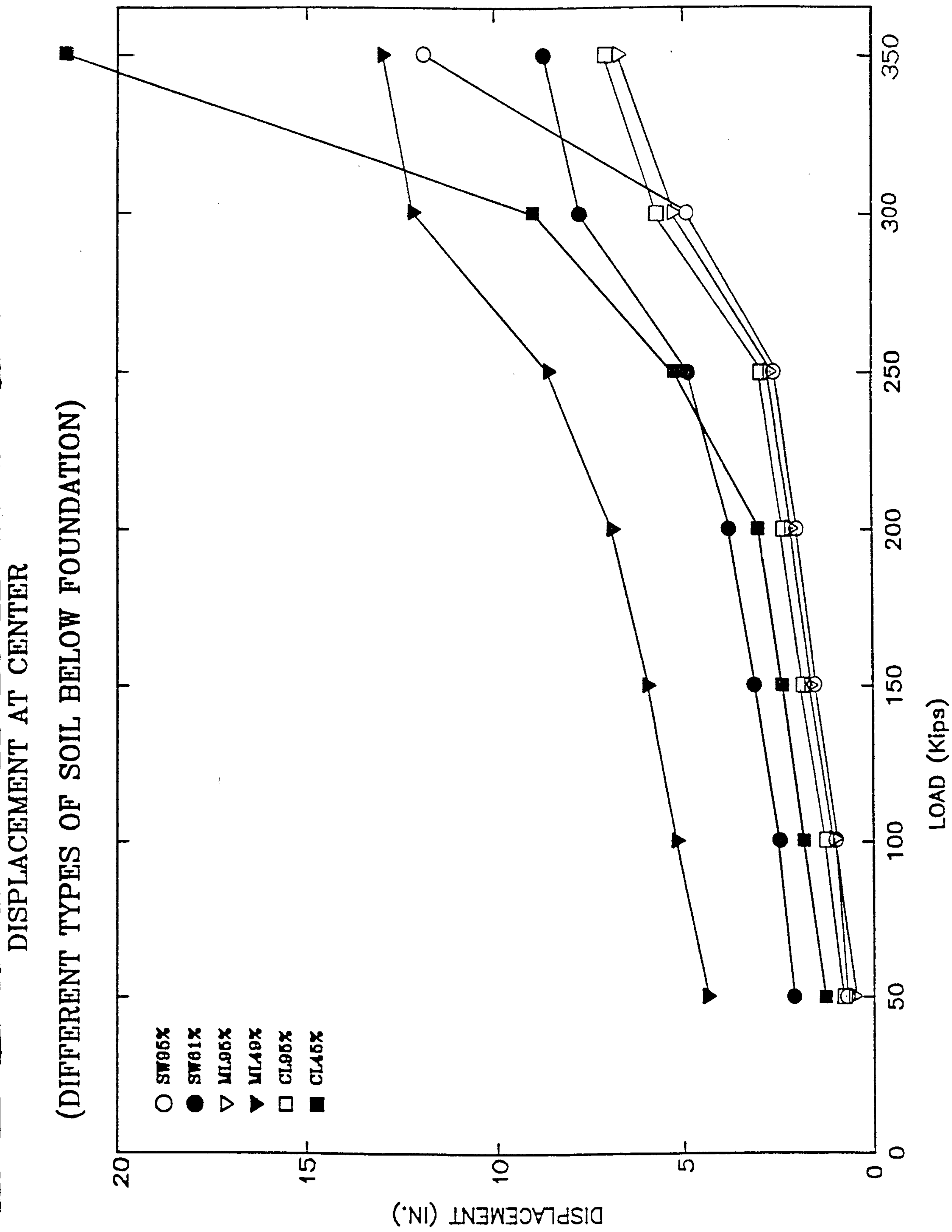

Figure 18

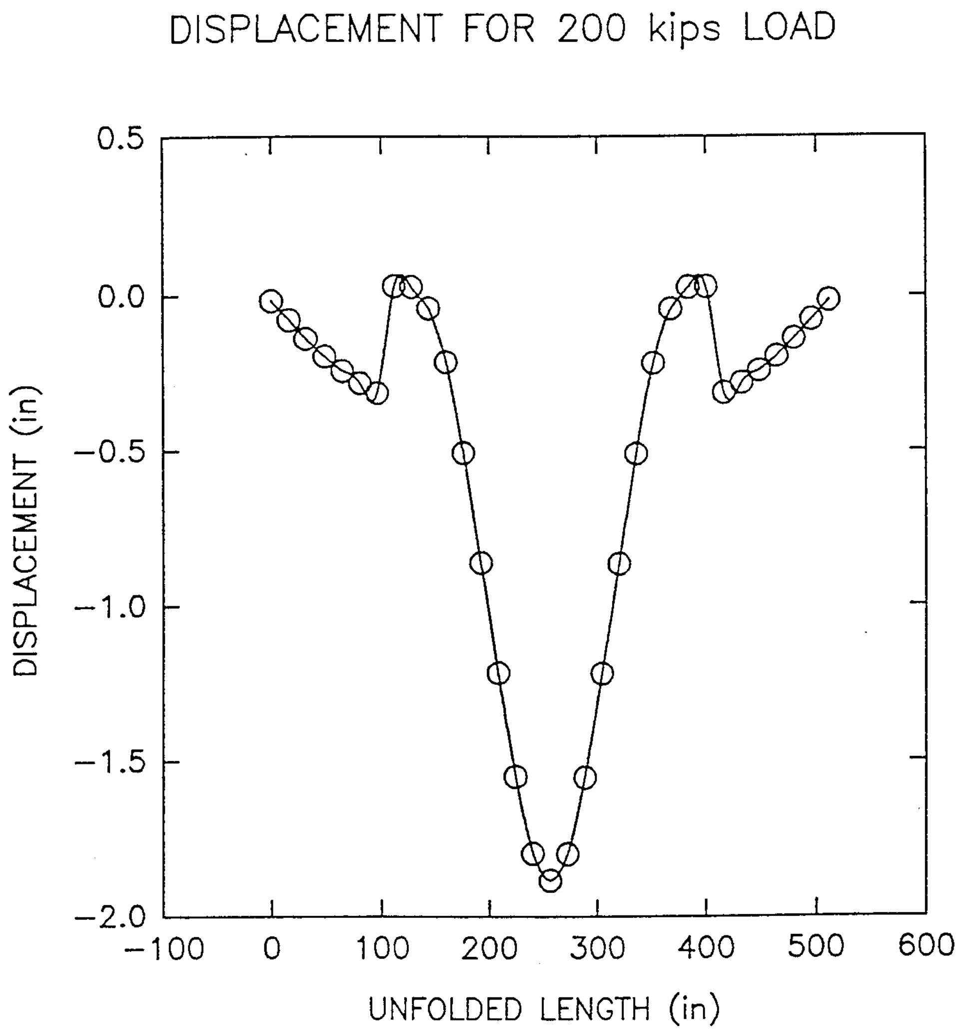

DISPLACEMENT FOR 200 kips LOAD
0.5
0.0
−0.5
−1.0
−1.5
−2.0
DISPLACEMENT (in)
−100
0
100
200
300
400
500
600
UNFOLDED LENGTH (in)

Figure 19

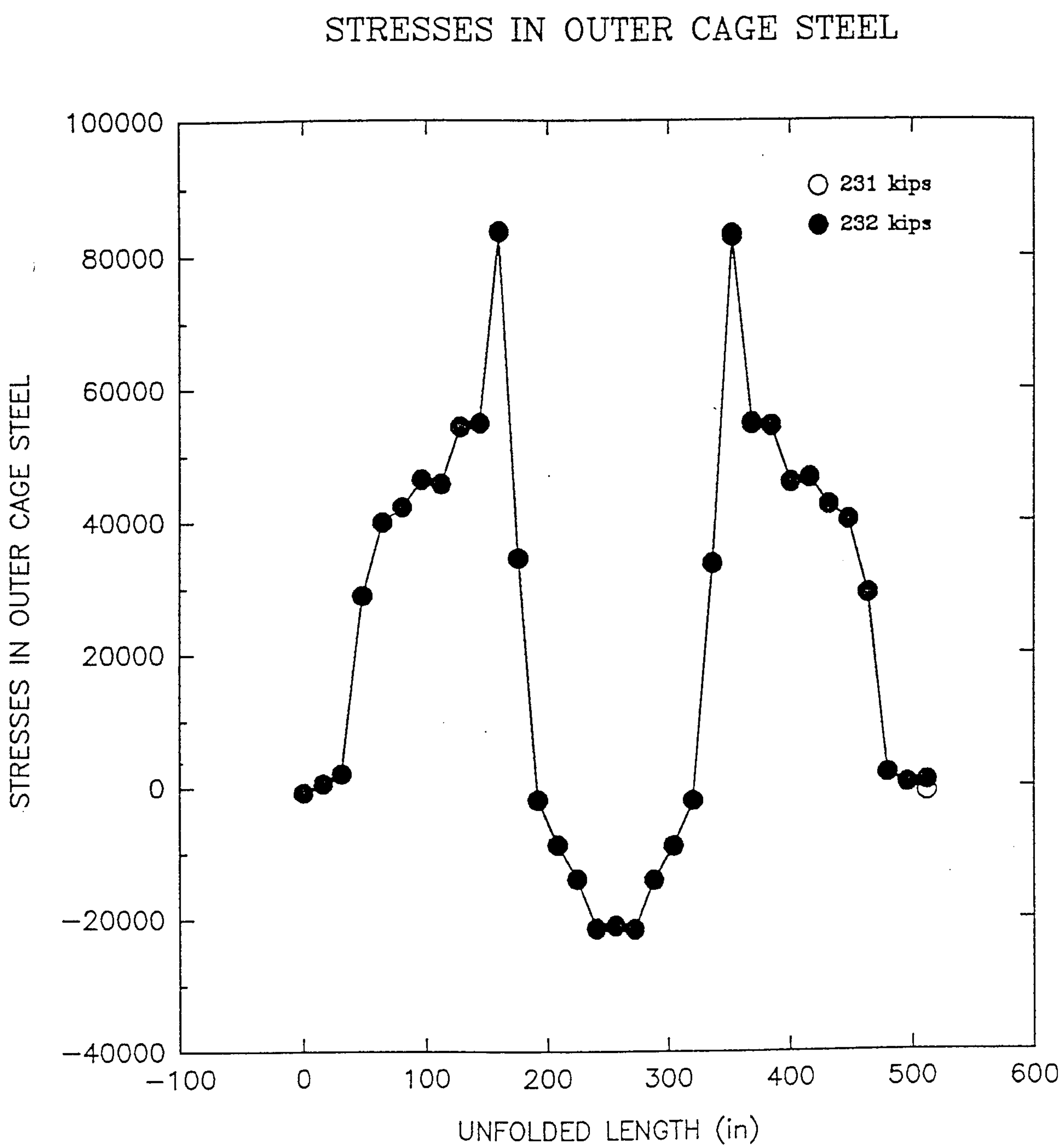
STRESSES IN OUTER CAGE STEEL
231 kips
232 kips
STRESSES IN OUTER CAGE STEEL
UNFOLDED LENGTH (in)
100000
80000
60000
40000
20000
0
−20000
−40000
−100
0
100
200
300
400
500
600

Figure 20

STRESSES IN INNER CAGE STEEL

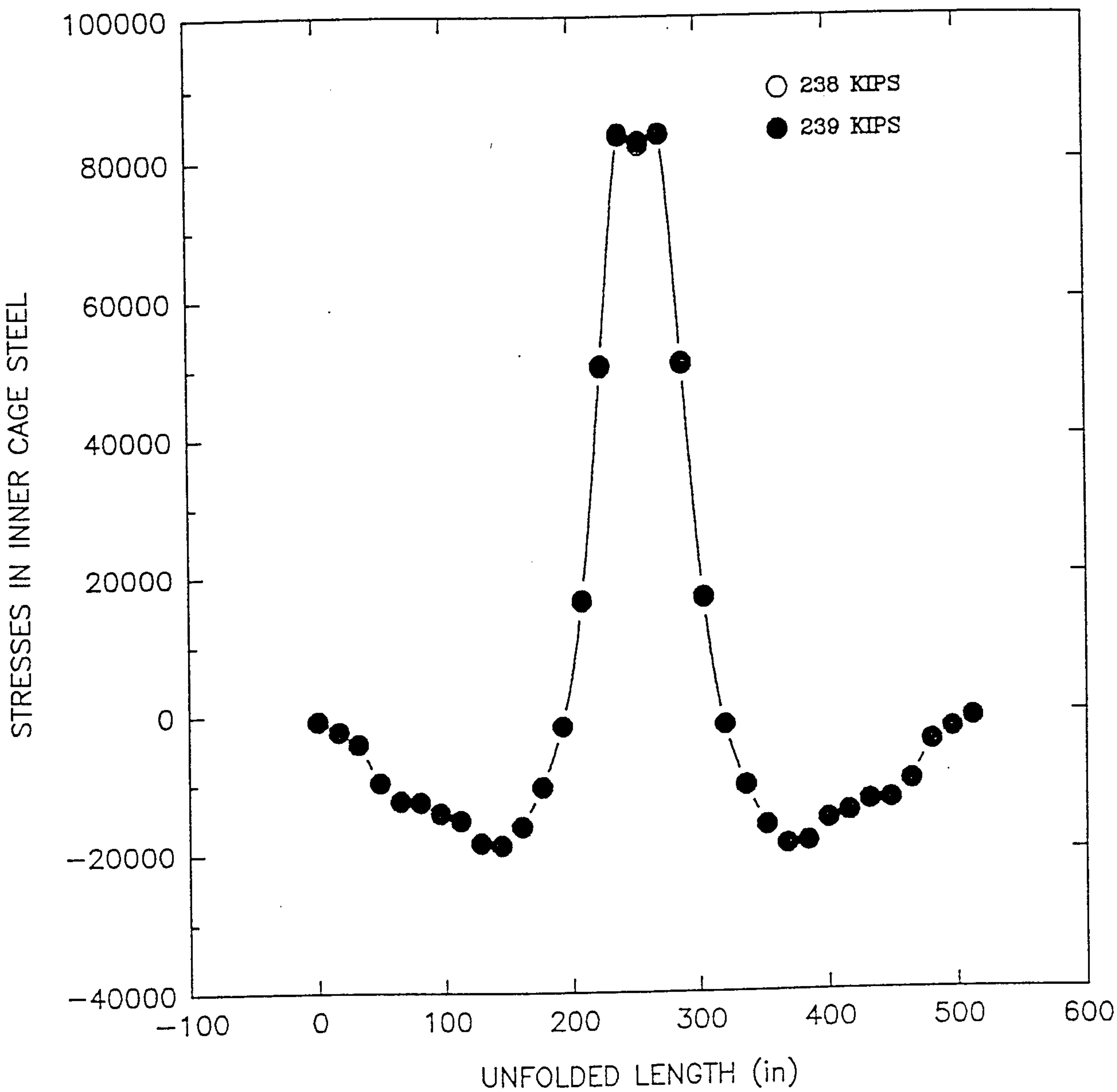

Figure 21

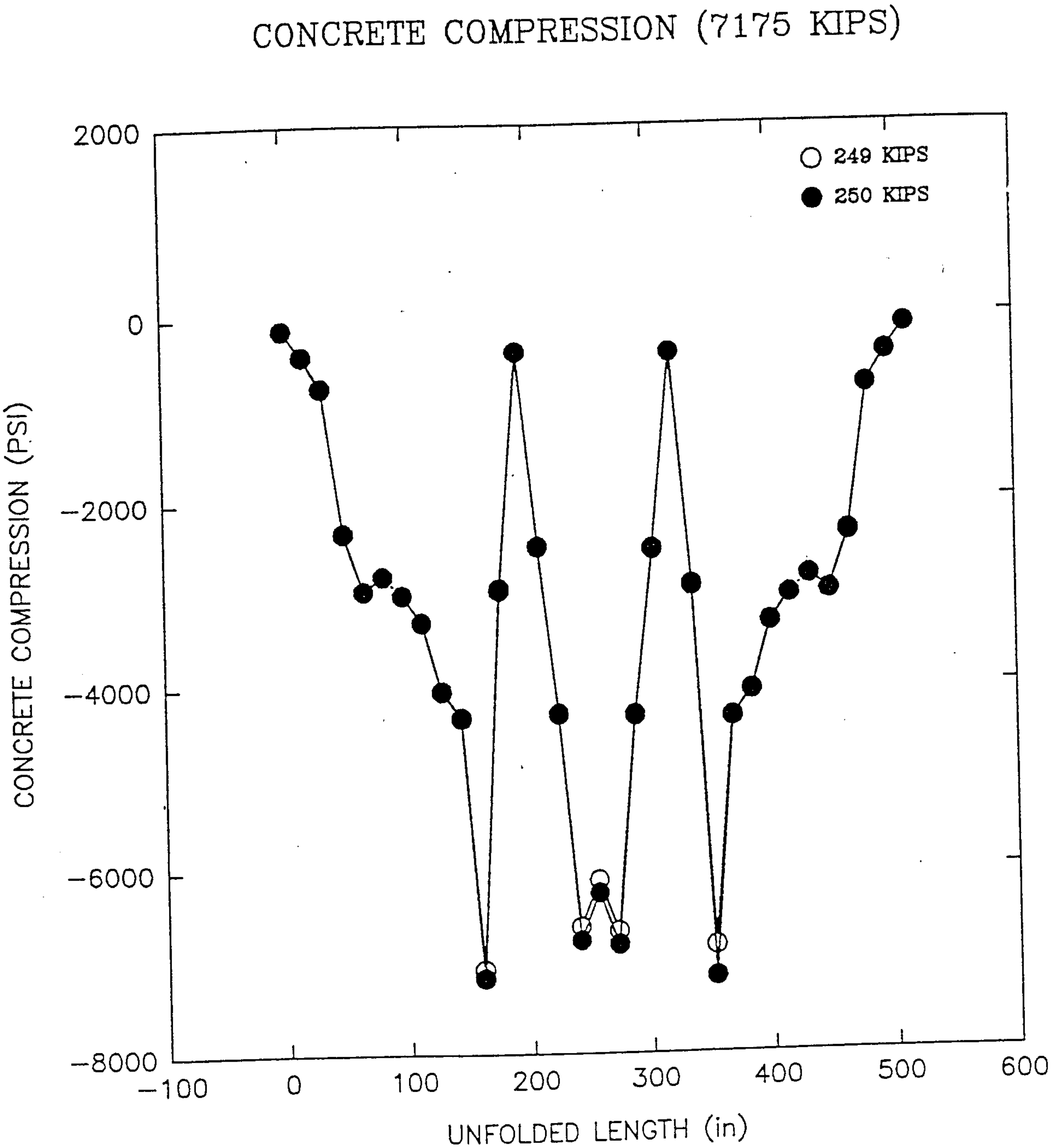
CONCRETE COMPRESSION (7175 KIPS)
249 KIPS
250 KIPS
CONCRETE COMPRESSION (PSI)
UNFOLDED LENGTH (in)
2000
0
−2000
−4000
−6000
−8000
−100
0
100
200
300
400
500
600

Figure 22

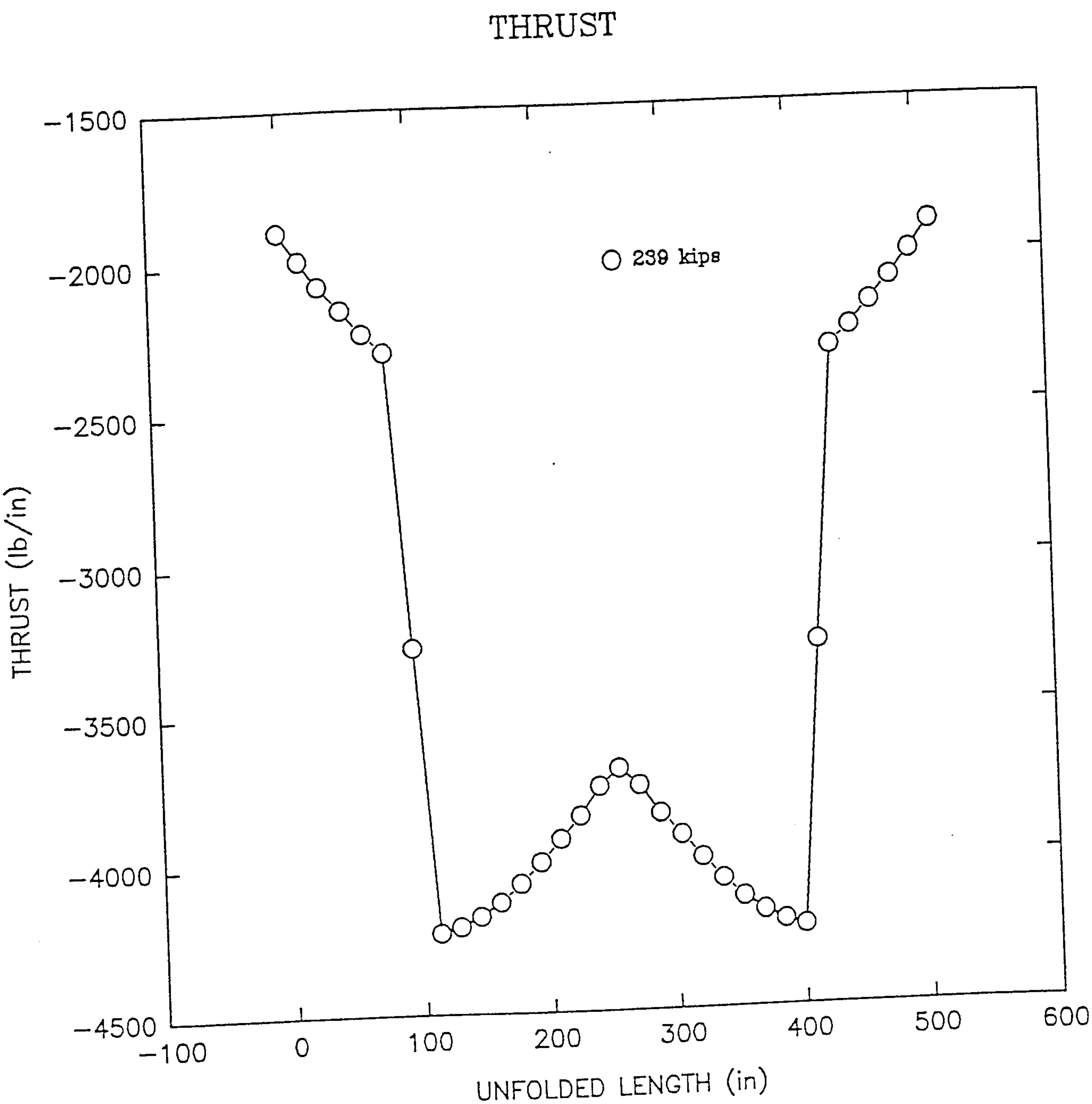
THRUST
239 kips
THRUST (lb/in)
-1500
-2000
-2500
-3000
-3500
-4000
-4500
-100
0
100
200
300
400
500
600
UNFOLDED LENGTH (in)

Figure 23

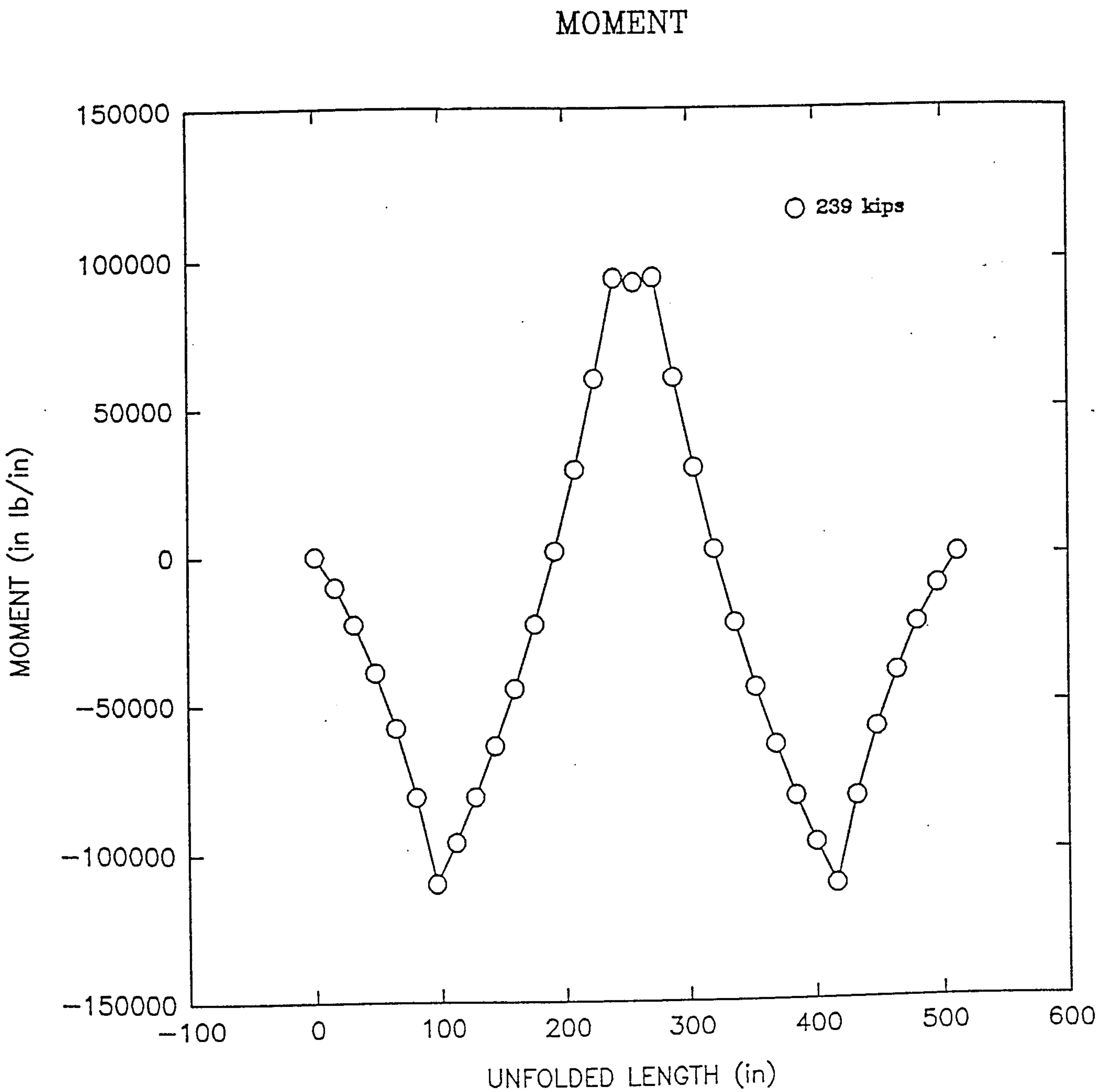
MOMENT
239 kips
150000
100000
50000
0
−50000
−100000
−150000
MOMENT (in lb/in)
−100
0
100
200
300
400
500
600
UNFOLDED LENGTH (in)

Figure 24

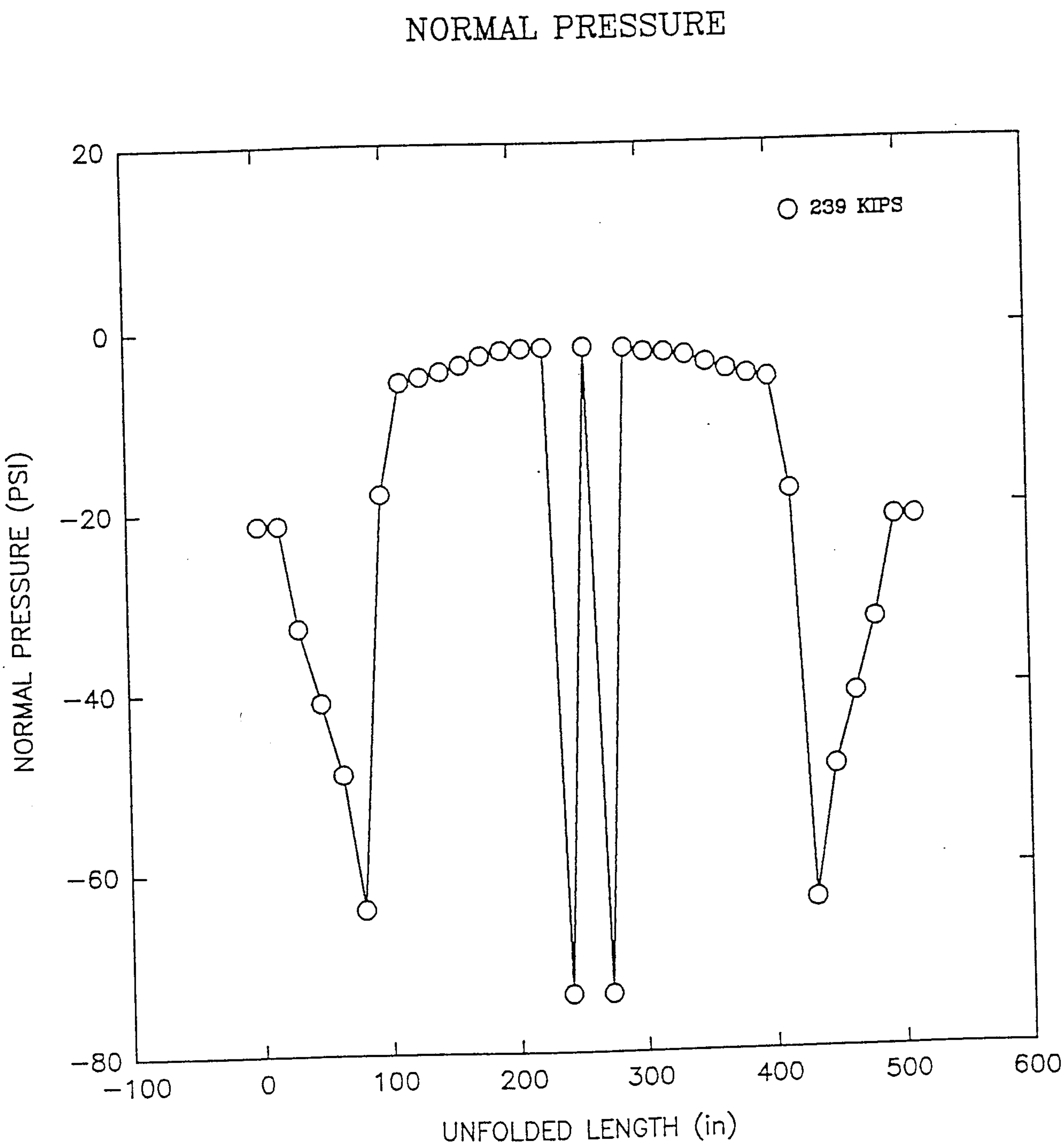
NORMAL PRESSURE
239 KIPS
20
0
-20
-40
-60
-80
-100
0
100
200
300
400
500
600
NORMAL PRESSURE (PSI)
UNFOLDED LENGTH (in)

Figure 25

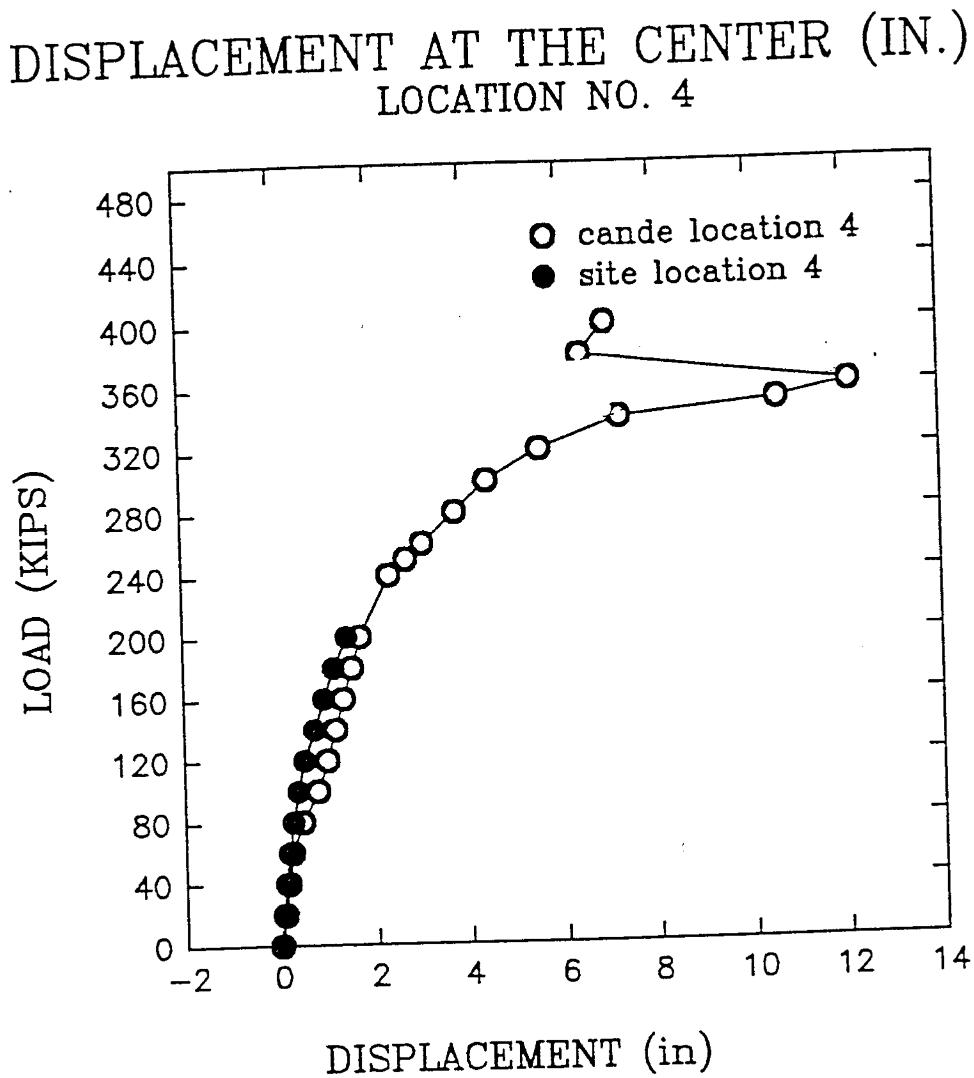
DISPLACEMENT AT THE CENTER (IN.)
LOCATION NO. 4
cande location 4
site location 4
LOAD (KIPS)
DISPLACEMENT (in)
480
440
400
360
320
280
240
200
160
120
80
40
0
-2
0
2
4
6
8
10
12
14

Figure 26

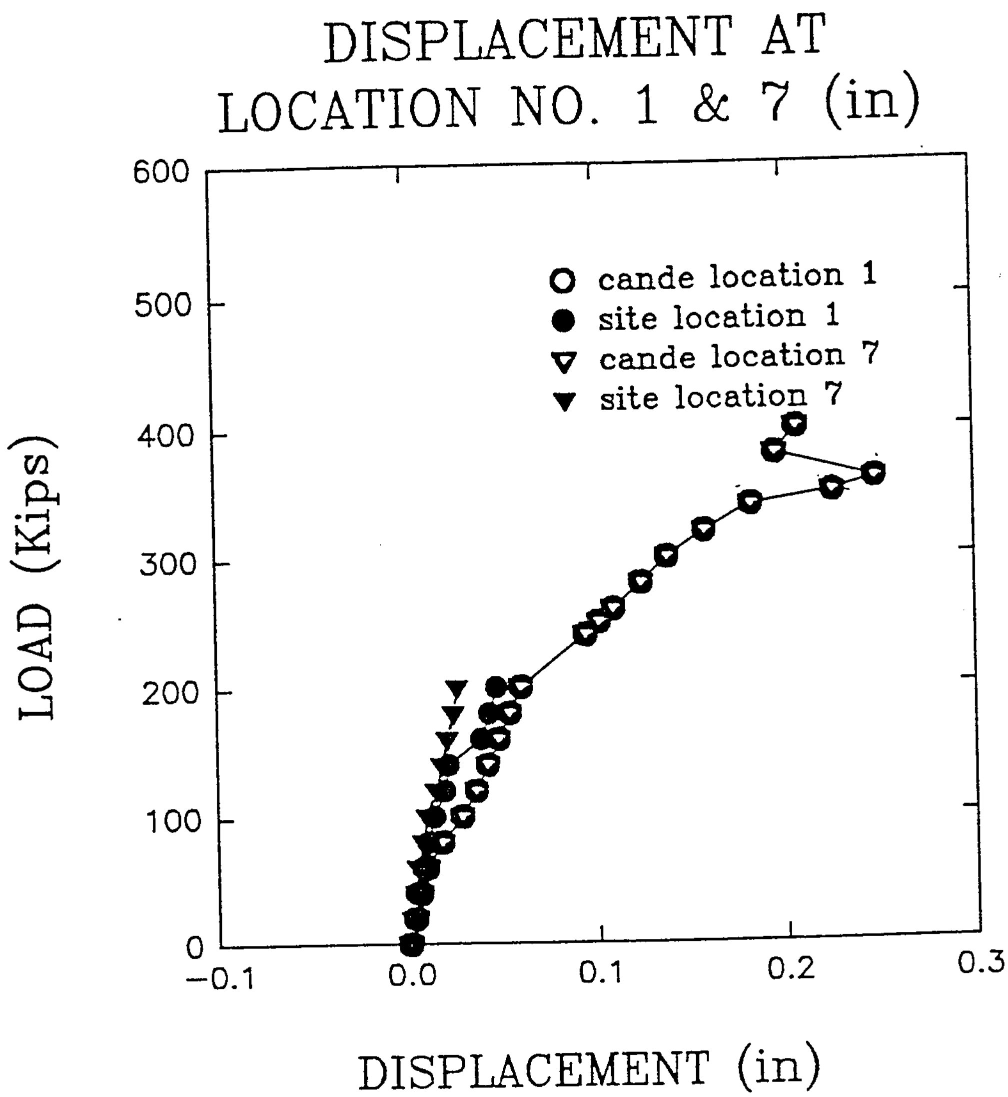
DISPLACEMENT AT
LOCATION NO. 1 & 7 (in)
cande location 1
site location 1
cande location 7
site location 7
LOAD (Kips)
600
500
400
300
200
100
0
−0.1
0.0
0.1
0.2
0.3
DISPLACEMENT (in)

Figure 27

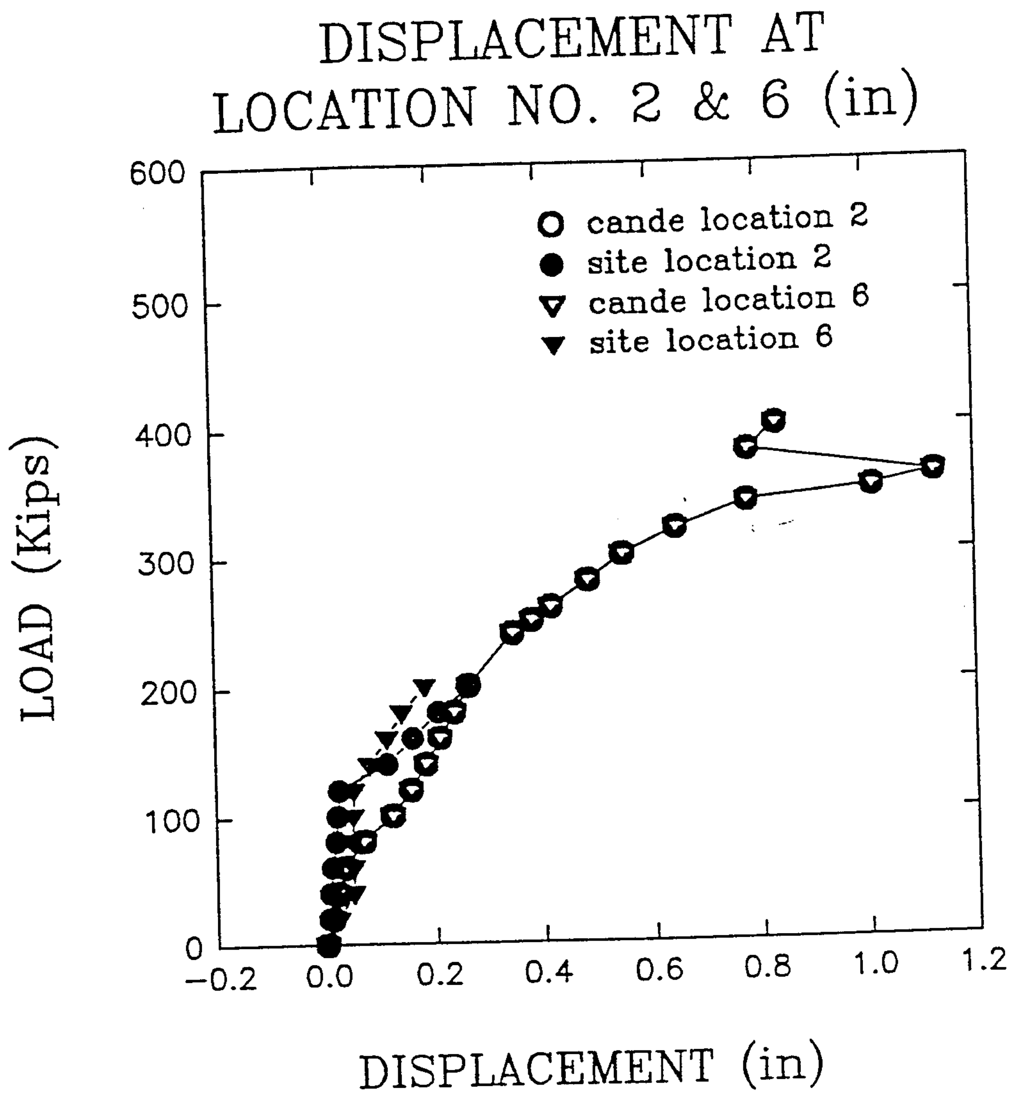
DISPLACEMENT AT
LOCATION NO. 2 & 6 (in)
cande location 2
site location 2
cande location 6
site location 6
LOAD (Kips)
DISPLACEMENT (in)
600
500
400
300
200
100
0
-0.2
0.0
0.2
0.4
0.6
0.8
1.0
1.2

Figure 28

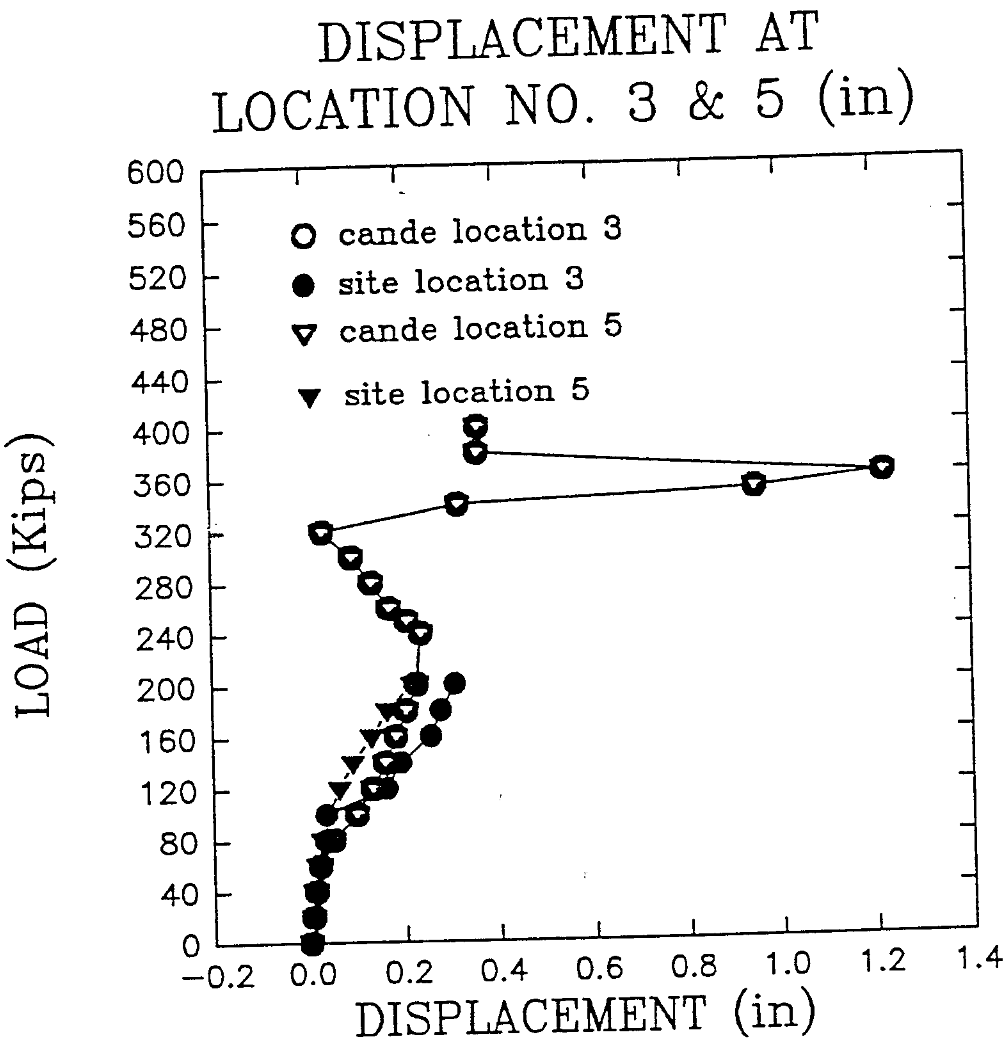
DISPLACEMENT AT
LOCATION NO. 3 & 5 (in)
cande location 3
site location 3
cande location 5
site location 5
LOAD (Kips)
DISPLACEMENT (in)
600
560
520
480
440
400
360
320
280
240
200
160
120
80
40
0
−0.2
0.0
0.2
0.4
0.6
0.8
1.0
1.2
1.4

Figure 29

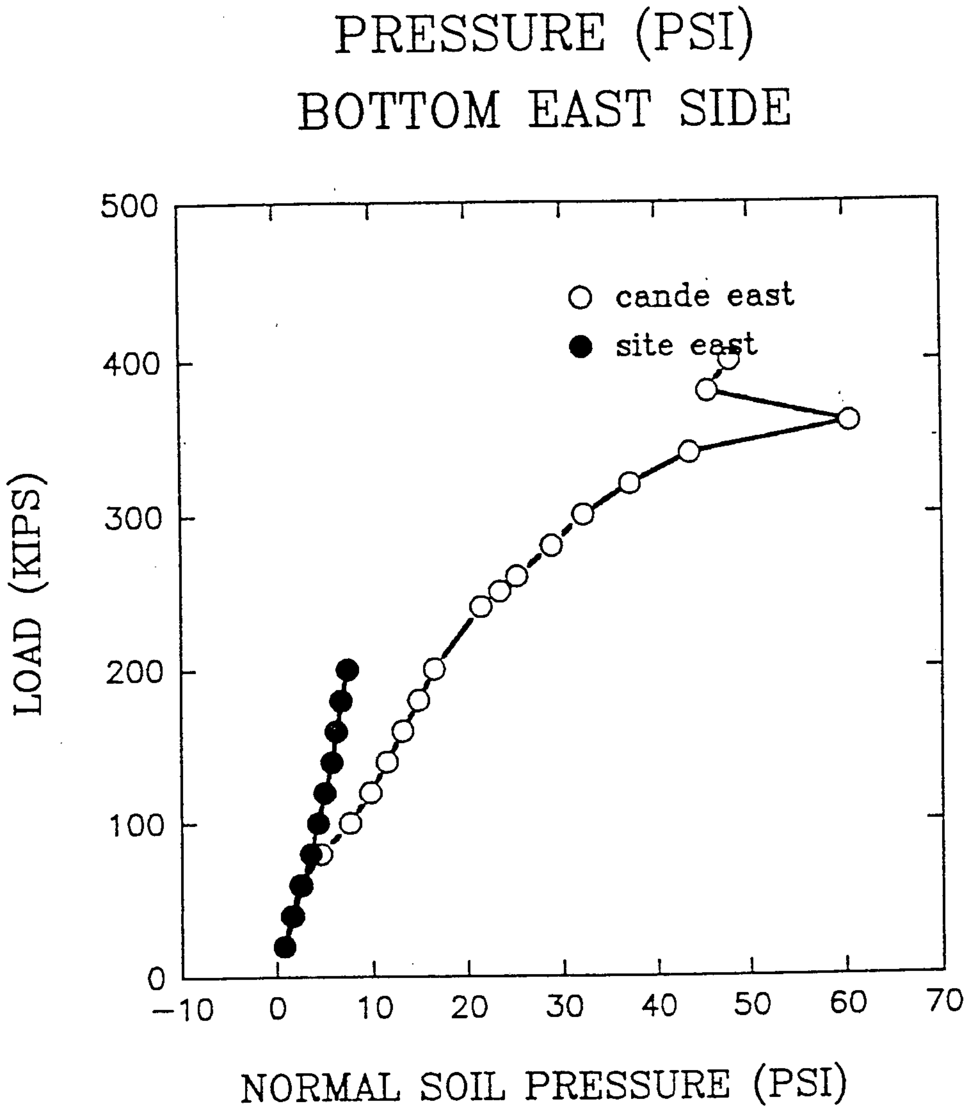
PRESSURE (PSI)
BOTTOM EAST SIDE
cande east
site east
LOAD (KIPS)
500
400
300
200
100
0
−10
0
10
20
30
40
50
60
70
NORMAL SOIL PRESSURE (PSI)

Figure 30

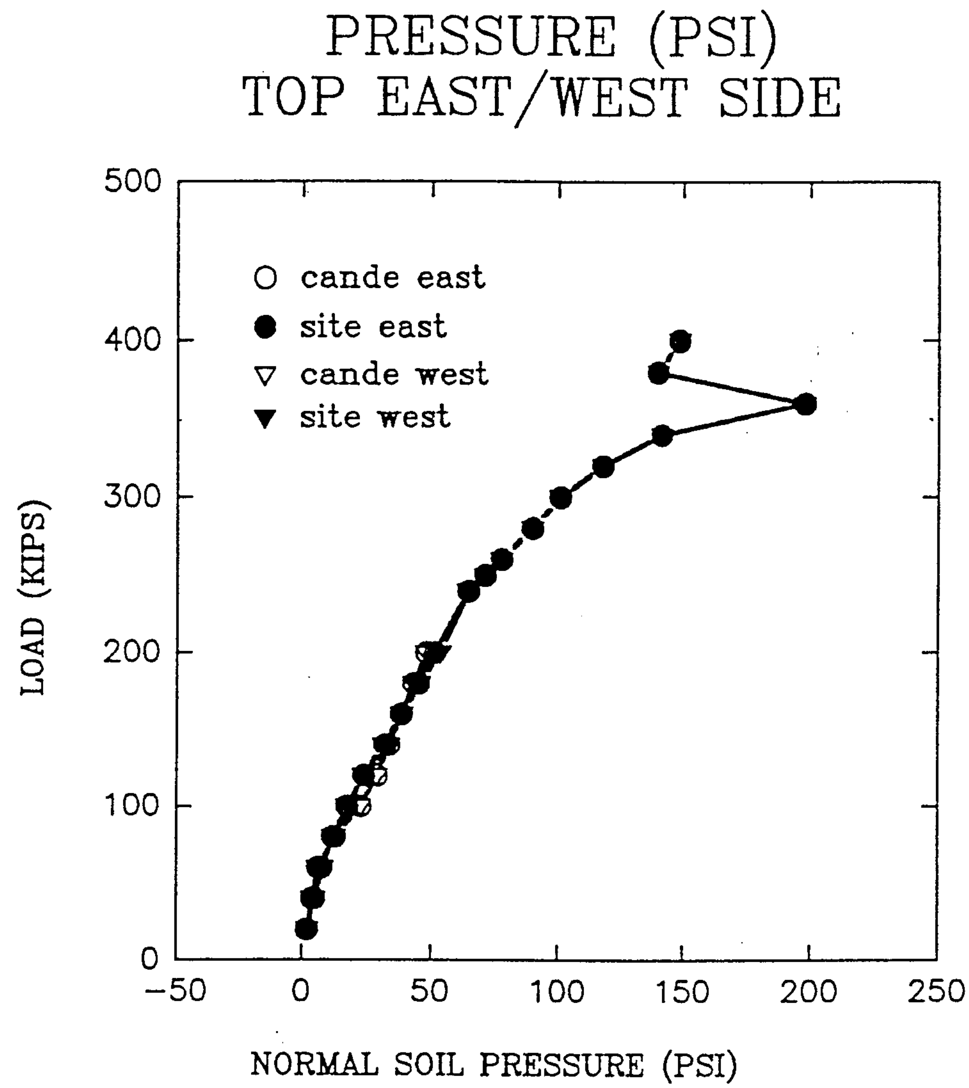
PRESSURE (PSI)
TOP EAST/WEST SIDE
cande east
site east
cande west
site west
LOAD (KIPS)
NORMAL SOIL PRESSURE (PSI)
500
400
300
200
100
0
-50
0
50
100
150
200
250

Figure 31

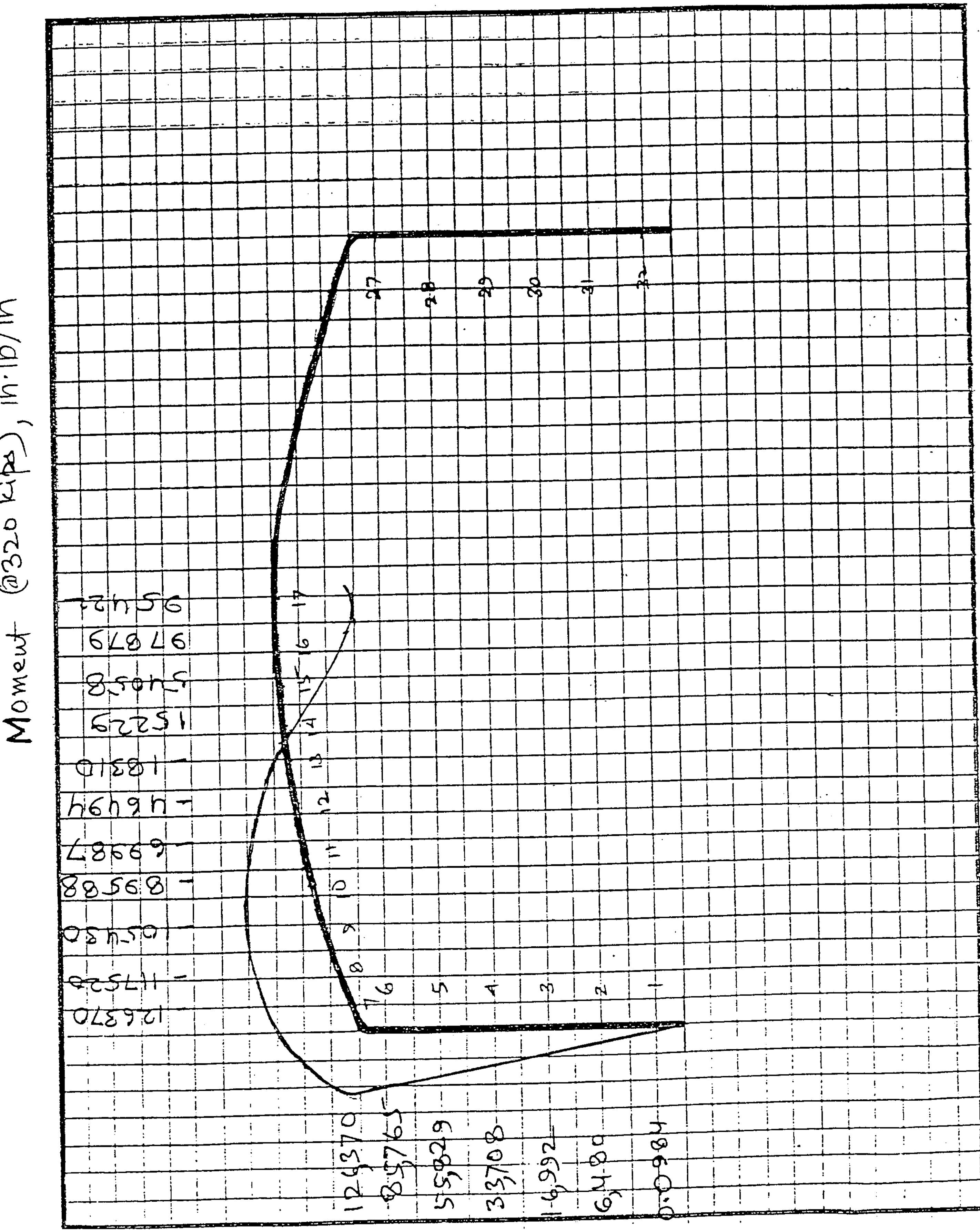
Moment (@320 kips), in·lb/in
126370
85765
55829
33708
16992
6480
0.0984

Figure 32